American Mineralogist, Volume 85, pages 1239–1254, 2000

The tremolite-actinolite-ferro–actinolite series: Systematic relationships among cell parameters, composition, optical properties, and habit, and evidence of discontinuities

JENNIFER R. VERKOUTEREN[1,*] AND ANN G. WYLIE[2]

[1]Chemical Sciences and Technology Laboratory, National Institute of Standards and Technology, Gaithersburg, Maryland 20899, U.S.A.
[2]Laboratory for Mineral Deposits Research, Department of Geology, University of Maryland, College Park, Maryland 20742, U.S.A.

ABSTRACT

Unit-cell parameters, optical properties, and chemical compositions have been measured for 103 samples in the tremolite-actinolite-ferro-actinolite series. The average values of the non-essential constituents are: ^{T}Al = 0.10(11), ^{C}Al = 0.06(6), ^{B}(Fe, Mn, Mg) = 0.09(7), ^{B}Na = 0.04(5), ^{A}Na = 0.09(9), and Cr, Ti, and K ≅ 0. Asbestiform actinolite samples have lower Al contents than massive or "byssolitic" actinolite samples. Unit-cell parameters for end members tremolite and ferro-actinolite based on regressions of the data are: a = 9.841 ± 0.003 Å, 10.021 ± 0.011 Å; b = 18.055 ± 0.004 Å, 18.353 ± 0.018 Å; c = 5.278 ± 0.001 Å, 5.315 ± 0.003 Å; and cell volume = 906.6 ± 0.5 Å^3, 944 ± 2 Å^3. The changes in a, b, and cell volume with ferro-actinolite substitution are modeled with quadratic functions, and the change in c with ferro-actinolite substitution is modeled with a linear function. There is a positive correlation between c and Al that results in a discrimination between asbestiform and massive or "byssolitic" habits for c and for the refractive indices. The principal refractive indices n_γ and n_β are linear with respect to ferro-actinolite substitution, but n_α is best modeled by two lines with a change in slope between 26 and 32% ferro-actinolite. Birefringence and extinction angle also change between 26 and 32% ferro-actinolite. The predicted end-member values of the principal refractive indices for tremolite and ferro-actinolite are: n_α = 1.602 ± 0.001, 1.661 ± 0.005; n_β = 1.621 ± 0.001, 1.692 ± 0.004; and n_γ = 1.631 ± 0.001, 1.700 ± 0.003. There is a discontinuity in a at approximately 11% ferro-actinolite that is accompanied by a drop in Ca. There are also indications of discontinuities in optical properties and c between 26 and 32% ferro-actinolite that may be due to an increase in tschermakite substitution. Both discontinuities are accompanied by a decrease in the relative frequency of natural samples.

INTRODUCTION

The tremolite-actinolite-ferro-actinolite series (the actinolite series, for short) is regulated, when asbestiform, by the Environmental Protection Agency (U.S. EPA 1987). The regulation applies only to fibers that fit the compositional definition of the actinolite series (Leake et al. 1997), and that exhibit optical and crystallographic properties that are not inconsistent with the general knowledge. The actinolite series is ideally $\square Ca_2(Mg, Fe, Mn)_5Si_8O_{22}(OH)_2$, and is subdivided on the basis of ferro-actinolite content [(Fe + Mn)/(Fe + Mn + Mg)] into tremolite (0–10% ferro-actinolite), actinolite (10–50% ferro-actinolite), and ferro-actinolite (50–100% ferro-actinolite). Common substitutions in the series can be described by the charge- and site-balanced exchange components $^{T}Si_{-1}{}^{A}\square{}^{T}Al_1{}^{A}Na_1$ (edenite), $^{T}Si_{-1}{}^{C}(Mg, Fe, Mn)_{-1}{}^{T}Al_1{}^{C}Al_1$ (tschermakite), $^{B}Ca_{-1}{}^{B}(Fe, Mg, Mn)_1$ (cummingtonite-grunerite), $^{B}Ca_{-1}{}^{A}\square{}^{B}Na_1{}^{A}Na_1$ (richterite), and $^{B}Ca_{-1}{}^{C}(Mg,Fe)_{-1}{}^{B}Na_1{}^{C}Al_1$ (glaucophane). The limits on compositional variability are given in Leake et al. (1997), and chemical analyses for over 100 natural samples are available in the literature. Dorling and Zussman (1987) analyzed a large set of samples in the actinolite series to compare compositional variability for asbestiform vs. non-asbestiform samples, and determined that the asbestiform habit correlates with lower Al contents. There is a suggestion of an ubiquitous cummingtonite-grunerite component in the actinolite series (Evans and Yang 1998). This point was first raised by analogy with synthetic tremolites, which are very difficult to synthesize on-composition and tend to have approximately 10% $Mg_2Mg_5Si_8O_{22}(OH)_2$ in solid solution (Jenkins 1987; Graham et al. 1989; Hawthorne 1995; Jenkins et al. 1997). A review by Jenkins (1987) of 25 published tremolite analyses concluded that natural tremolite is deficient in Ca with respect to C-site cations (C = $^{[6]}$Al, Mg, Fe, Mn, Cr, Ti), although Graham et al. (1989) pointed to published analyses of tremolite with ideal Ca/∑C ratios. Synthetic tremolite has an excess of Mg equivalent to the deficiency in Ca and an otherwise ideal composition, and therefore the argument of a systematic cummingtonite solid solution is well grounded. Hawthorne (1995) questioned the use of Ca/∑C as an indicator of cummingtonite-grunerite solid solution in natural tremolite samples, as it is only appropriate when other types of substitutions have been considered and when ^{C}Mg > 5 atoms per formula unit (apfu).

Tremolite, actinolite, and ferro-actinolite are $C2/m$ clinoamphiboles, and recent X-ray structural refinements are found in Yang and Evans (1996) and Evans and Yang (1998). Yang and Evans (1996) compared a near end-member tremolite to synthetic tremolite, and concluded that an 8–10% cummingtonite component in tremolite results in a unit-cell volume decrease from 907.0 Å^3 to 904.2 Å^3, and a decrease in β from 104.76° to ~104.55°. Synthetic tremolite has an a di-

*E-mail: Jennifer.verkouteren@nist.gov

mension consistently smaller than the value of 9.836 Å given by Yang and Evans (1996) for natural tremolite, although the *b* and *c* dimensions are similar (e.g., Pawley et al. 1993; Smelik et al. 1994; Jenkins et al. 1997). Evans and Yang (1998) reported a linear increase in *a*, *b*, *c*, and unit-cell volume with ferro-actinolite content, although the data for *a*, *b*, and unit-cell volume deviate systematically from the predicted values. The deviations are attributed to variable amounts of cummingtonite-grunerite component, Al, and F, even though the samples used by Evans and Yang (1998) were selected to conform as closely as possible to compositional ideality. Correlations between elemental substitutions and lattice dimensions have been postulated based on differences among end-member amphiboles in natural (Papike et al. 1969) and synthetic (Colville et al. 1966; Ernst 1968) samples, and from measurements of synthetic amphiboles on the relevant binary joins tremolite-tschermakite (Smelik et al. 1994; Jenkins et al. 1997), tremolite-richterite (Pawley et al. 1993), and tremolite-potassium-richterite (Hawthorne et al. 1997). These studies can provide general information, but cannot be used to predict the range in values expected for the lattice parameters in the actinolite series.

Measurements of the optical properties of tremolite, actinolite, and ferro-actinolite are available in the literature, and significant compilations are found in Winchell (1945), Winchell (1963), and Deer et al. (1997). In all cases, the correlation between refractive index and ferro-actinolite content was modeled with a linear function, although a linear function is required only for the case of a vibration direction parallel to a symmetry axis (Winchell 1945), as is the case for the *Y* direction. There are significant deviations in the data from the linear models presented in each study, and all the models suffer from lack of data for ferro-actinolite. The values of n_α and n_γ given for the tremolite end-member, for which there are several natural samples, vary within ± 0.004 among Winchell (1945), Winchell (1963), and Deer et al. (1997). Winchell (1963) provides the only values for n_β for the tremolite and ferro-actinolite end-members, although an n_β for synthetic ferro-actinolite is provided by Ernst (1966). Extinction angle is thought to decrease with increasing ferro-actinolite content (Phillips and Griffen 1981; Nesse 1991; Deer et al. 1997), although Winchell (1963) gives calculated end-member extinction angles of 16.2° for tremolite and 32.1° for ferro-actinolite. The extinction angle measurements compiled by the various sources exhibit significant deviations from a linear model with a negative slope: the highest extinction angle (24°) listed in Deer et al. (1997) occurs at 28% ferro-actinolite, significantly higher than the predicted tremolite end-member value of 16°. There is no distinction made in the compilations of optical properties between asbestiform and non-asbestiform samples, and presumably, although habit is rarely mentioned, the results apply to non-asbestiform samples. The asbestiform habit is known to induce significant changes to the optical properties of a mineral species as a result of the fibrillar nature of asbestos and the inability, in many cases, to resolve individual fibers (Heinrich 1965; Wylie 1979). The optical properties observed from composite fiber bundles indicate a higher symmetry than for individual fibers, and observed changes for asbestiform grunerite (amosite) include parallel extinction rather than inclined extinction, and 2 indices of refraction (n'_α and n'_γ) rather than 3 (NIST 1991).

The goal of our study was to analyze a sufficient number of samples to assess the range in lattice dimensions and optical properties for the compositional variability allowed within the definition of the actinolite series as given in Leake et al. (1997). In this manner, any fibrous sample can be unambiguously identified for the purposes of the regulation. Our data set contains chemical composition (Na, K, Si, Al, Ca, Mg, Fe, Mn, Cr, Ti), cell parameters (*a*, *b*, *c*, β, unit-cell volume), optical properties (n_α, n_β, n_γ, extinction angle $Z \wedge c$), and habit (asbestiform, "byssolitic"[1], massive) for 103 samples that span the range from the tremolite end-member to 87% ferro-actinolite. Principal component analysis was used to determine correlations among chemical composition, optical properties, and unit-cell dimensions within the actinolite series. Earlier uses of principal component analysis were concerned only with chemical correlations across groups of amphiboles (Saxena and Ekström 1970). The large number of samples and the combination of data allowed us to address many issues of current interest about the actinolite series, including the question of Ca deficiency, the systematic presence of a cummingtonite component, and the influence of chemical variation on cell parameters. In addition, new information is provided on differences due to habit, and chemical and structural discontinuities in the series.

Experimental methods

Sample selection and characterization

Samples were obtained from museums, universities, and private individuals, and were selected on the basis of microprobe results following the general classification given by Leake et al. (1997): specifically, $^{B}(Ca + Na) \geq 1.00$, $^{B}Na < 0.50$, $^{A}(Na + K) < 0.50$, and $Si \geq 7.50$. The habit of each sample was characterized as asbestiform, "byssolitic," or massive (Table 1). Samples identified as asbestos have a silky luster and occur in bundles of very thin, flexible fibers that are easily separable by hand pressure. The asbestiform samples were ground with great difficulty, often matting in the mortar. The term "byssolitic" was applied to samples that occur as single fibers, sometimes loosely aligned, that have a vitreous luster and are easily reduced to a powder by hand grinding. Individual "byssolitic" fibers are often tabular in cross-section with well-developed (100) faces and widths of at least a few micrometers. The term massive was applied to all other habits. Within this group, samples ranged from acicular to almost equidimensional cleavage fragments.

[1]Despite recommendations by the IMA (Leake 1978) to remove the term byssolite, considered as synonymous with asbestos, the term has been adopted by the asbestos community to describe a stiff, fibrous variety of amphibole, following Dana (1932), that is *not* asbestiform. Because this remains an important distinction with respect to regulatory terminology, the term "byssolitic" has been retained for this paper.

Microprobe analysis

Samples were embedded in epoxy, polished for microprobe analysis, and analyzed by using a JEOL JXA-8600[2] electron microprobe and energy dispersive spectrometry. The data were collected at 20 kV and 0.75 nA for 200 s. Elemental concentrations were determined by using matrix corrections (ZAF) from Desktop Spectrum Analyzer (Fiori and Swyt 1994) and the following standards: NIST glass K412 from SRM 470 (Mg, Al, Si, Ca, Fe) (Marinenko 1982), Kakanui hornblende (Na, K, Ti) (source = Smithsonian, E. Jarosewich), fayalite (Mn) (source = Smithsonian, J. Nelen) and Johnstown hypersthene (Cr) (source = Smithsonian, J. Nelen). The concentrations of F and Cl were not determined. The uncertainty in the measurement of the major elements is within ±5% relative, as determined by analysis of standard specimens (Table 2). Elemental concentrations were converted to oxides based on stoichiometry, assuming all Fe as Fe^{2+}. The results were considered acceptable if the total oxides summed to 95% or greater, although a few analyses with totals between 92 and 95% were included if the results were reproducible and followed the site occupancy constraints given below. The results for each sample (Table 3) represent an average of between 2 and 6 analyses. Elemental concentrations were converted to apfu on the basis of 23 oxygen atoms. Cations were assigned after Hawthorne (1981) to four basic group-sites based on the general formula $A_{0-1}B_2C_5T_8O_{22}(OH)_2$, where T-type cations (Si and Al) occur at the two independent tetrahedral sites (T1 and T2); C-type cations (Al, Mg, Fe, Mn, Cr, Ti) occur at the three independent octahedral sites (M1, M2, and M3); B-type cations (Fe, Mn, Mg, Ca, Na) are surrounded by eight anions at the M4 site; and A-type cations (Na, K) are surrounded by up to 12 anions. Sites were filled in the order recommended by Leake et al. (1997). Site occupancy constraints constituted an additional criterion for acceptance of an analysis based on the following limits: Si ≤ 8.05 apfu, Σ (Si, Al) ≥ 7.90 apfu, Σ (Si, Al, Ti, Cr, Fe, Mg, Mn) ≥ 12.90 apfu, Σ (Si, Al, Ti, Cr, Fe, Mg, Mn, Ca) ≤ 15.10 apfu, and Σ (Si, Al, Ti, Cr, Fe, Mg, Mn, Ca, Na) ≥ 14.90 apfu.

X-ray diffraction

Samples were prepared for powder X-ray diffraction (XRD) by hand-grinding followed by dispersal in water, deposition of the slurry on a glass slide, and drying at low temperature. An internal Si standard (NIST SRM 640b) was added to the sample in the grinding stage. The data were collected by using Cu$K\alpha$ radiation generated at 40 kV and 55 mA on a Philips PW1800 diffractometer equipped with theta-compensating slit and a diffracted beam graphite monochromator. The angular collection range was 5–100° 2θ with a step size of 0.02° 2θ and a scan time of 4 s/step. The data were corrected for specimen displacement by using the internal standard, and peak positions and intensities were determined by fitted profiles by using Jade for Windows (Materials Data 1995). Cell parameters (*a*, *b*, *c,* and β) and their associated 1σ uncertainties (Table 1) were determined from approximately 40 of the most intense reflections (normally > 3% I/I_0) by using the APPLEMAN unit-cell refinement program (Philips Electronic Instruments Co. 1991a). The cell refinement and indexing results were compared to standard patterns of tremolite, actinolite, and ferro-actinolite and to model patterns generated by POWDER (Philips Electronic Instruments Co. 1991b) for similar compositions by using lattice position assignments from Mitchell et al. (1971) and by assuming preferred orientation parallel to [001]. Acceptance of the cell refinement required convergence of the program, correspondence of predicted and true peak positions within ±0.03° 2θ, and general agreement with the model pattern of the expected intensities and Miller indices.

Optical properties

Refractive index measurements were performed with a spindle stage (Bloss 1981) at a range of wavelengths to calculate the index at 589.3 nm (n_D) (Table 1). Individual fibers or cleavage fragments were mounted on glass fibers and oriented with the goniometer such that the direction of elongation (*c* axis) remained parallel to the privileged direction of the lower polarizer during rotation. The principal vibration directions were located by rotation about the *c* axis to find the position of parallel extinction, which is unique to (100) and contains the *Y* vibration direction. The (010) plane containing n_α, n_γ, and extinction angle was found by a 90° rotation about the *c* axis from (100). The uncertainties in the refractive index measurements are controlled primarily by the dispersion of the immersion liquids (Verkouteren et al. 1992), and for these measurements the standard uncertainties are ±0.001 or better.

We were able to measure principal refractive indices for 19 of the 35 asbestiform samples by orientation of individual fibers, as described above. The fibers on which the measurements were performed had widths ≥2 μm, and therefore are wider than most of the asbestiform fibers. Although it is possible that the measured fibers are not representative of the more common, very-fine fibers, they do not appear to be different in index of refraction based on Becke-line comparisons in grain mounts. The remaining 16 asbestiform samples had anomalous optical properties indicative of a fibrillar structure (Heinrich 1965; Wylie 1979), and for these samples we were able to determine the maximum (n'_γ) and minimum (n'_α) indices of refraction parallel and perpendicular to elongation. Values of n'_γ and n'_α predicted from twinning models or simple averages bore no simple relationship to the measured values, and this phenomenon, along with other complex features such as the absence of extinction on (010) for some "byssolitic" samples, require a full discussion and are treated in a separate publication (Verkouteren and Wylie in preparation).

Results and discussion

Cummingtonite-grunerite substitution

To address the question in the literature concerning a systematic cummingtonite-grunerite component in the actinolite

[2]Certain commercial equipment, instruments, or materials are identified to specify adequately the procedure. Such identification does not imply recommendation or endorsement by the National Institute of Standards and Technology, nor does it imply that the materials or equipment identified are necessarily the best available for the purpose.

TABLE 1. Sample localities, cell parameters, and optical properties and samples are sorted by ferro-actinolite content [(Fe + Mn/Fe + Mn + Mg) = X_{FeA}]

SC	X_{FeA}	*a* (Å)	*b* (Å)	*c* (Å)	β°	*V* (Å^3)	n_α	n_β	n_γ	$c\wedge Z$	$2V_Z$*	H	color
216	0.1	9.837(1)	18.048(1)	5.278(1)	104.67(1)	907	1.599	1.615	1.627	16.4	97.5	M	wh
193	0.3	9.844(1)	18.057(1)	5.277(1)	104.75(1)	907	1.603	1.623	1.631	16.8	112.6	M	wh
249	0.4	9.843(1)	18.062(2)	5.280(1)	104.72(1)	908	1.603	1.621	1.632	15.9	106.0	M	wh
48	0.6	9.847(1)	18.059(1)	5.276(1)	104.75(1)	907	1.601	1.618	1.630	16.4	101.7	A	wh
29	0.7	9.850(1)	18.063(1)	5.272(3)	104.76(2)	907	1.600	1.617	1.628	15.8	104.8	A	wh
213	0.9	9.841(1)	18.059(1)	5.278(1)	104.74(1)	907	1.603	1.622	1.632	15.7	108.8	B	wh
240	0.9	9.843(1)	18.059(2)	5.279(1)	104.77(1)	907						M	wh
239	1.0	9.845(1)	18.056(1)	5.277(1)	104.75(1)	907	1.604	1.622	1.633	15.8	105.8	B	v lt gn
247	1.1	9.830	18.047	5.277	104.64	906	1.602	1.617	1.631	15.6	95.3	M	wh
231	1.1	9.845(1)	18.055(1)	5.276(1)	104.75(1)	907	1.603	1.620	1.631	15.7	103.9	A	wh
194	1.2	9.826(1)	18.053(2)	5.276(1)	104.69(1)	905	1.605	1.622	1.632	15.8	108.4	M	apple gn
250	1.4	9.838(1)	18.054(2)	5.279(1)	104.67(1)	907	1.601	1.618	1.630	16.0	101.9	M	wh
144	1.5	9.843(1)	18.060(2)	5.280(1)	104.77(1)	908	1.605	1.624	1.633	15.0	112.4	A	lt tan
128	1.5	9.846(1)	18.058(2)	5.280(1)	104.78(1)	908	1.604	1.621	1.633	17.0	101.9	B	wh
61	2.5	9.842(1)	18.064(1)	5.279(1)	104.74(1)	908						B	wh
9	2.6	9.841(1)	18.057(1)	5.278(1)	104.76(1)	907	1.604	1.622	1.632	16.5	104.2	A	wh
198	2.6	9.849(1)	18.054(2)	5.279(1)	104.76(1)	908	1.605	1.622	1.632	15.8	106.6	M	lt gn
31	2.8	9.843(1)	18.060(1)	5.279(1)	104.75(1)	907	1.604	1.621	1.632	16.0	102.6	B	wh
226	3.0	9.835(1)	18.058(1)	5.279(1)	104.69(1)	907						A	lt tan
147	3.3	9.842(1)	18.048(2)	5.280(1)	104.84(1)	907	1.608	1.625	1.635	15.9	105.6	M	lt gn
185	3.3	9.849(1)	18.064(2)	5.279(1)	104.75(2)	908	1.604	1.622	1.633	16.1	105.7	A	wh
138	3.4	9.845(1)	18.063(2)	5.277(1)	104.75(1)	908	1.608	1.625	1.636	15.7	105.2	B	gold
37	3.5	9.847(1)	18.066(1)	5.280(1)	104.76(1)	908						A	lt tan
146	3.6	9.845(1)	18.067(2)	5.285(3)	104.76(1)	909	1.605	1.625	1.633	16.0	114.5	M	lt gn
15	3.9	9.852(1)	18.060(1)	5.276(1)	104.72(1)	908	1.606	1.623	1.633	15.1	107.0	B	wh
254	4.2	9.843(1)	18.063(1)	5.278(1)	104.75(1)	908	1.606	1.623	1.634	16.6	101.8	A	v lt gn
8	4.6	9.846(1)	18.067(1)	5.279(1)	104.74(1)	908	1.605	1.623	1.633	15.7	104.9	B	wh
248	4.7	9.844(1)	18.067(2)	5.276(1)	104.72(1)	905	1.606	1.624	1.634	15.7	106.0	A	lt tan
204	4.9	9.847(1)	18.060(2)	5.278(1)	104.73(1)	908	1.609	1.625	1.635	16.0	102.7	M	gn
30	5.1	9.846(1)	18.064(1)	5.285(1)	104.76(1)	909		1.619				B	lt gn
184	5.2	9.851(1)	18.058(2)	5.280(1)	104.76(1)	908	1.605	1.621	1.632	17.8	101.4	M	dk gn
238	5.4	9.834(1)	18.061(1)	5.281(1)	104.67(1)	907						A	lt tan
242	5.5	9.839(1)	18.064(2)	5.281(1)	104.70(1)	908						A	lt tan
155	5.5	9.847(1)	18.067(1)	5.279(1)	104.75(1)	908	1.605		1.633	15.2		A	wh
229	6.1	9.831(1)	18.065(1)	5.280(1)	104.64(1)	907	1.609	1.626	1.637	16.0	102.9	B	lt tan
47	6.3	9.854(1)	18.066(2)	5.277(1)	104.71(1)	909	1.608	1.624	1.636	16.7	101.1	B	v lt gn
199	6.4	9.828(1)	18.032(1)	5.278(1)	104.52(1)	906	1.613	1.628	1.637	15.8	106.4	M	gn
52	6.4	9.851(1)	18.072(1)	5.282(1)	104.75(1)	909	1.607	1.624	1.635	16.2	103.8	B	wh
14	6.5	9.833(1)	18.068(2)	5.281(1)	104.65(1)	908	1.607	1.623	1.634	16.0	102.9	A	wh
140	6.6	9.850(1)	18.073(1)	5.282(1)	104.75(1)	909						A	lt gn
49	7.3	9.827(1)	18.063(3)	5.280(3)	104.61(2)	907	1.608	1.624	1.636	16.2	99.9	B	wh
245	7.6	9.848(1)	18.076(1)	5.279(1)	104.73(1)	909	1.610	1.626	1.637	15.7	100.6	M	v lt gn
232	7.7	9.846(1)	18.071(1)	5.278(1)	104.73(1)	908	1.609	1.626	1.636	16.7	104.2	M	lt gn
214	7.8	9.846(1)	18.071(1)	5.280(1)	104.72(1)	909	1.609	1.625	1.635	15.6	105.4	A	wh
143	7.9	9.848(1)	18.068(1)	5.279(1)	104.75(1)	908	1.606	1.623	1.632	16.0	108.6	A	wh
43	8.2	9.844(1)	18.074(3)	5.279(1)	104.72(1)	908	1.606	1.622	1.633	17.1	103.5	M	gn
46	8.6	9.855(2)	18.081(3)	5.278(3)	104.79(3)	909						A	gn
154	8.9	9.839(1)	18.069(1)	5.283(1)	104.69(1)	909	1.609	1.626	1.637	15.9	102.6	A	lt tan
148	9.1	9.849(1)	18.060(2)	5.277(1)	104.64(1)	908	1.612	1.628	1.638	17.2	101.8	B	lt gn
208	10.5	9.846(1)	18.081(2)	5.280(1)	104.67(1)	909	1.611		1.638	15.8		B	v lt gn
202	10.9	9.841(1)	18.061(2)	5.284(1)	104.66(1)	909	1.615	1.631	1.639	16.0	107.5	M	dk gn
157	11.9	9.829(1)	18.068(1)	5.283(1)	104.69(1)	907	1.613	1.629	1.640	15.7	102.0	M	dk gn
224	12.1	9.831(1)	18.073(1)	5.283(1)	104.66(1)	908	1.616	1.633	1.643	16.2	103.7	M	gn
206	12.2	9.829(1)	18.072(1)	5.283(1)	104.64(1)	908	1.617	1.631	1.642	17.7	98.3	M	dk gn
210	12.8	9.827(1)	18.074(1)	5.284(1)	104.66(1)	908	1.616	1.631	1.642	16.6	97.1	M	dk gn
205	13.3	9.819(1)	18.054(2)	5.288(1)	104.68(1)	907						M	dk gn
187	13.5	9.825(1)	18.063(1)	5.285(1)	104.67(1)	907	1.617	1.633	1.643	16.5	103.3	M	dk gn
246	13.8	9.836(1)	18.063(1)	5.284(1)	104.66(1)	908	1.617	1.631	1.641	16.0	104.6	M	dk gn
156	14.6	9.833(1)	18.060(1)	5.284(1)	104.63(1)	908	1.620	1.636	1.645	16.3	106.5	M	dk gn
160	14.6	9.830(1)	18.070(2)	5.287(2)	104.69(2)	908	1.615	1.629	1.641	16.0	96.2	M	dk gn
129	14.7	9.847(1)	18.088(2)	5.282(1)	104.69(1)	910				16.9		A	lt gn

Notes: SC = Sample numbering code. H = habit: M = massive, B = "byssolitic," A = asbestiform. Color: wh = white, gn = green, bn = brown. Source: S = Smithsonian Institution, H = Harvard Mineral Musuem, USBM = U.S. Bureau of Mines, AMNH = American Museum of Natural History, JM = Johns Mansville, VPI = Virginia Polytechnic Institute and State University, NIST SRM= National Institute of Standards and Technology Standard Reference Material. Others are names of individuals mentioned in acknowledgements.

* $2V_Z$ calculated from measured refractive indices.

TABLE 1—*Extended*

Source	Locality
	Gouverneur, NY
	Cockeysville, MD
	Canaan Co. CT, Pfitzer Quarry
S 101747, D-338	Gugeris Quarry, Line Pits, Lancaster Co. PA
	India
	Unknown
	Marriottsville Quarry, Cockeysville Formation, Carroll County, MD
	Quebec
	Balmat, NY
	Easton, PA
	St. Lawrence Co, NY
	Unknown
Davis	Korea
	Unknown
S 102839	Pylesville, MD
S 8536	Parkton, MD
H 124281	Gooderham, Ontaria
S 118117	Jenkins Farm near Pylesville, Harford County, MD
C.S. Thompson	CA
Davis	Shinness Loch Shin, NW Lairg, Ross and Cromarty, Scotland
NIST	Bastica, Corsica
	Muncaster Road, Laytonsville MD
S C2535-1	Pusterthol, Tyrol, Austria
Davis	Carr Brae Dornie, Inverness-shire, N.W. Scotland
S 135167	Heiligenblut, Australia
NIST SRM1867	Conda deposit, Barstow, CA
S c2534	Harz Mountains, Germany
J. Furman	MD
H 118211	Hadwood Lake, Ontaria Canada
S C2531	Taberg, Sweden
NIST SM-1 135811	Nordland, Ontaria Canada
C.S. Thompson	CA
	Montgomery Co. MD, Shady Grove Area n. of Rt. 28
Davis	Col D'Isera S. of Val D'Isere, France
VPI M1000	Wytheville, VA
S 16343	Rabinal, Baja, Verapaz, Guatemala
H 80474	Mineral Hill, PA, Delaware Co.
S 46308	New South Wales, Australia
	Udaipur District, Rajasthan State, India
	Rt. 28 at Quince Orchard, Montgomery Co. MD
H 98761	Mina D'Saphira, Portugal
	Montgomery Co. MD, Shady Grove Area n. of Rt. 28
	Montgomery Co. MD, associated with massive serpentine
	Rockville, MD
BNHM 4173-70-6 (Davis)	Jamestown, CA
S 16583	Baltimore, MD
S 85880	Loudon County, VA
	Darnestown, VA
Davis	Ala d'Stura, N.W. Italy
	Fairfax, VA
H 116209	Berryessa Canyon near San Jose, Santa Clara Co. CA
S R11396	Karnten Austria
	Mineral Hill, Carroll Co. MD
H 126840	Pfitschergrund, Pfitsch, Tyrol, Austria
	Enoree, SC
H 126841	Lisens, Tyrol, Austria
Ward's 4GW0350	San Bernadino Co. CA
	CA
S 139355	Sonoma County, CA
S 85884	Near Morava, Czechoslovakia at Vernorovice, Sobotin
	Fairfax, VA

—*Continued next page*

series, we chose to look at several compositional and site-occupancy factors. Deficiencies in ^{B}Ca from 2 apfu can be due to ^{B}(Mg, Fe, Mn) or to ^{B}Na. The large number of samples in our study allows us to look at these compositional factors independently and draw some conclusions concerning cummingtonite-grunerite substitution in the actinolite series.

The mean value of ^{B}Ca is 1.89(9) apfu, although a mean is not the best statistic to use as the distribution is skewed and the mode is closer to the ideal of 2 apfu. Most of the samples display some Ca deficiency, although some samples have ideal, or close to ideal ^{B}Ca. There is, on average, an excess of C-type cations, with a mean value of excess C of 0.09(7) apfu. However, the excess of C-type cations is not due primarily to Mg + Fe + Mn > 5 apfu, as the mean value of this sum is 5.02(8) apfu. A better way to look at the sum of Mg + Fe + Mn is through the linear relationship represented by the substitution of Fe and Mn for Mg (Fig. 1). The intercept is 4.98(4) Fe + Mn apfu and the slope is –0.99(1). The total range in Fe + Mn + Mg is 5.0 ± 0.2 apfu, with the residuals randomly distributed for 0–30% ferro-actinolite (Fig. 1). (The residuals are generally negative for 30–50% ferroactinolite, and positive for 50–90% ferroactinolite.)

The remaining cation that must be considered in evaluating excess C is ^{C}Al, as Cr and Ti are present above detection limits in only 16 of the 103 samples, and therefore can be ignored in a general discussion of site occupancies. There is a linear relationship between Al and Si (Fig. 2), and the substitutional mechanism falls between an ideal edenite (slope of –1, but no ^{C}Al) and an ideal tschermakite substitution (slope of –2, some ^{C}Al). This substitutional mechanism results in ^{C}Al > 0 on average, with a mean value of 0.06(6) apfu. Because of the order in which the sites are filled, the combination of ^{C}Al > 0 and Fe + Mn + Mg ≅ 5 apfu results in ^{B}(Mg, Fe, Mn) > 0, which means there must be, on average, a cummingtonite-grunerite component. The Al vs. Si and Fe + Mn vs. Mg substitutions are associated, as the residuals from the two linear regressions are correlated negatively such that positive Fe + Mn vs. Mg residuals (Fe + Mn + Mg > 5) are associated with negative Al vs. Si residuals (lower ^{C}Al). Thus, the average value of excess C does not change with the amount of ^{C}Al or with ferro-actinolite content; it is half the value given for synthetic tremolite (excess C = 0.2 apfu) (Jenkins 1987; Graham et al. 1989; Hawthorne 1995; Jenkins et al. 1997). Natural samples also exhibit a range in excess C that includes zero, which is different from the reports on synthetic tremolites.

Unit-cell parameters

Unit-cell parameters *a*, *b*, *c*, (and volume) correlate most strongly with ferro-actinolite content, as indicated in the principal component analysis (Fig. 3) by the positive correlation of those parameters with Fe. The changes in the *a* and *b* dimensions and unit-cell volume are not linear with respect to ferro-actinolite content, but are better modeled by quadratic functions (Figs. 4a and 4b). Quadratic equations calculated for the data of Evans and Yang (1998) for *a*, *b*, and unit-cell volume are within the 95% confidence intervals calculated for the regressions of our data. The scatter in the two sets of data for *a*, *b*, and unit-cell volume also appear to be similar based on the

TABLE 1—*Continued*

SC	X_{FeA}	*a* (Å)	*b* (Å)	*c* (Å)	β°	*V* (Å^3)	n_α	n_β	n_γ	$c\wedge Z$	$2V_Z$*	H	color
192	14.8	9.822(1)	18.065(1)	5.285(1)	104.63(1)	907	1.619	1.634	1.645	18.0	99.5	M	gn
45	14.9	9.817(1)	18.063(2)	5.288(2)	104.64(1)	907	1.617	1.633	1.643	16.9	106.1	M	dk gn
207	15.0	9.827(1)	18.058(2)	5.286(1)	104.65(1)	908	1.622	1.636	1.645	17.0	101.6	M	dk gn
203	15.2	9.834(1)	18.057(1)	5.285(1)	104.63(1)	908	1.617	1.632	1.643	16.2	98.6	M	dk gn
25	15.4	9.857(1)	18.096(3)	5.287(2)	104.78(2)	912	1.616	1.632	1.642	15.8	104.9	M	lt gn
139	15.6	9.856(1)	18.088(2)	5.282(1)	104.73(1)	911	1.613		1.639			A	lt tan
253	15.7	9.852(1)	18.088(1)	5.283(1)	104.69(1)	911	1.613	1.629	1.639	15.9	103.0	A	v lt gn
141	15.9	9.844(1)	18.083(3)	5.280(1)	104.65(2)	909	1.615	1.632	1.641	16.6	109.5	M	gn
188	16.5	9.836(1)	18.087(3)	5.285(1)	104.65(2)	910							
153	17.0	9.841(1)	18.084(2)	5.285(1)	104.71(1)	910	1.615	1.631	1.642	15.5	101.6	M	dk gn
161	17.0	9.847(1)	18.081(2)	5.284(1)	104.63(1)	910	1.617	1.632	1.643	16.0	101.7	B	gn
255	17.4	9.854(1)	18.090(2)	5.285(1)	104.70(1)	911						A	gn
137	17.6	9.844(1)	18.089(1)	5.286(1)	104.65(1)	911						A	v lt gn
158	18.1	9.860(1)	18.077(2)	5.285(1)	104.74(2)	911	1.615		1.641	15.7		M	dk gn
163	18.7	9.841(1)	18.074(2)	5.288(1)	104.73(2)	910	1.622	1.637	1.648	15.5	99.5	M	dk gn
7	19.3	9.852(1)	18.095(1)	5.284(1)	104.67(1)	911	1.616	1.632	1.642	15.9	103.9	A	lt tan
200	19.7	9.859(2)	18.087(1)	5.281(4)	104.76(4)	911	1.624	1.637	1.648	19.3	96.9	M	dk gn
110	19.8	9.865(1)	18.110(2)	5.290(1)	104.79(1)	914	1.623	1.640	1.649	16.2	108.6	B	v lt gn
44	20.5	9.864(2)	18.088(3)	5.282(4)	104.82(2)	911	1.625	1.638	1.648	18.2	97.6	M	dk gn
151	21.0	9.852(1)	18.086(1)	5.289(1)	104.73(1)	911	1.623	1.640	1.649	16.9	108.6	B	gn
227	21.1	9.871(1)	18.115(1)	5.288(1)	104.76(1)	914						A	lt tan
72	25.8	9.865(1)	18.096(1)	5.291(1)	104.81(1)	913	1.626	1.638	1.648	18.4	96.3	M	dk gn
26	32.5	9.877(1)	18.134(2)	5.298(1)	104.76(1)	918	1.630	1.646	1.654	15.6	110.1	M	bn
159	33.4	9.862(1)	18.114(1)	5.305(1)	104.85(2)	916	1.629	1.645	1.655	14.0	104.0	M	gn
12	34.4	9.862(1)	18.112(1)	5.300(1)	104.76(1)	915		1.651				B	dk gn
235	35.6	9.868(1)	18.120(2)	5.295(1)	104.73(1)	916	1.630	1.645	1.655	15.7	102.1	A	dk gn
150	37.1	9.875(2)	18.136(6)	5.295(3)	104.73(3)	917						A	gn
225	38.1	9.880(1)	18.135(2)	5.296(1)	104.76(1)	918	1.631	1.648	1.656	14.9	110.4	M	gn
38	38.5	9.868(1)	18.116(2)	5.290(1)	104.71(1)	915						A	lt tan
201	40.7	9.883(1)	18.134(2)	5.296(1)	104.79(1)	918						B	gn
60	41.5	9.877(1)	18.125(2)	5.297(1)	104.80(1)	917	1.636	1.652	1.662	15.5	104.4	B	v lt gn
54	42.7	9.899(3)	18.194(12)	5.307(2)	104.71(4)	924	1.637		1.663	15.3		B	bn
162	44.7	9.872(1)	18.143(2)	5.304(1)	104.72(2)	919	1.638	1.656	1.663	14.5	116.7	M	dk gn
20	45.3	9.883(1)	18.151(1)	5.302(1)	104.78(1)	920	1.639	1.655	1.665	13.3	103.3	M	dk gn
109	49.1	9.895(4)	18.187(6)	5.302(3)	104.81(4)	923	1.639	1.657	1.665	14.4	112.0	B	bn
132	51.7	9.884(1)	18.145(2)	5.294(1)	104.70(2)	918						A	gn
149	57.1	9.902(1)	18.173(3)	5.299(1)	104.76(2)	922	1.642	1.661	1.670	14.7	114.0	A	gn
107	63.9	9.909(2)	18.185(4)	5.309(2)	104.66(3)	925	1.645		1.676	14.9		B	dk gn
66	70.2	9.927(1)	18.205(3)	5.305(1)	104.59(1)	928						A	lt gray
115	71.8	9.916(2)	18.232(4)	5.302(1)	104.51(2)	928						A	gn
164	77.8	9.965(5)	18.290(5)	5.301(7)	104.71(8)	935	1.656	1.678	1.687	13.8	115.9	M	gn
94	87.5	9.993(2)	18.296(5)	5.304(2)	104.81(2)	937	1.651	1.672	1.683	12.7	109.0	A	lt gray

Notes: SC = Sample numbering code. H = habit: M = massive, B = "byssolitic," A = asbestiform. Color: wh = white, gn = green, bn = brown. Source: S = Smithsonian Institution, H = Harvard Mineral Musuem, USBM = U.S. Bureau of Mines, AMNH = American Museum of Natural History, JM = Johns Mansville, VPI = Virginia Polytechnic Institute and State University, NIST SRM = National Institute of Standards and Technology Standard Reference Material. Others are names of individuals mentioned in acknowledgements.
* $2V_Z$ calculated from measured refractive indices.

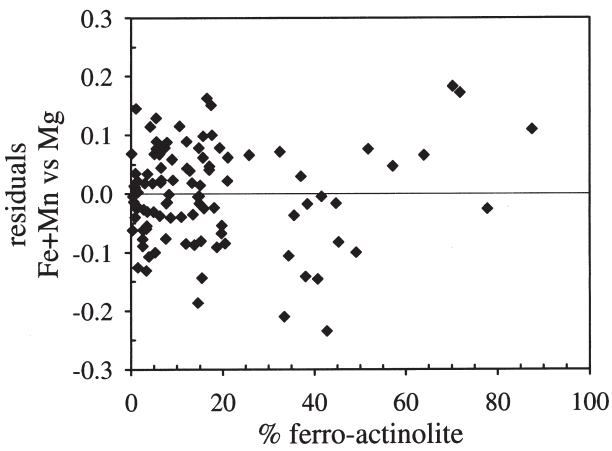

FIGURE 1. Residuals from the fit of Fe + Mn vs. Mg (R^2 = 0.99) plotted vs. the ferro-actinolite content.

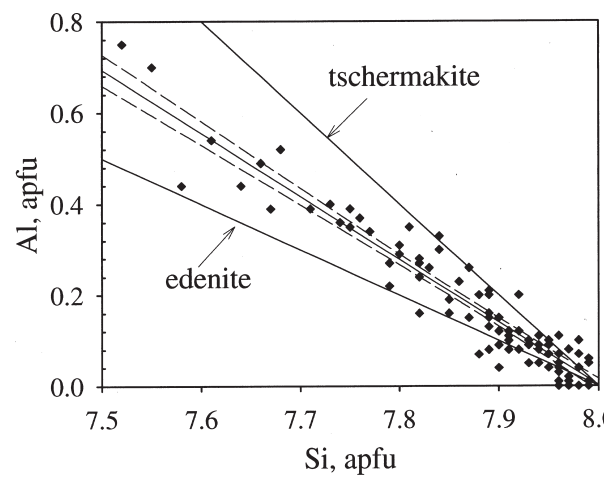

FIGURE 2. Linear regression of Al vs. Si, R^2 = 0.91. Dashed lines represent 95% confidence limits on the regression. Solid lines show the trends for edenite and tschermakite substitutions.

TABLE 1—*Extended*

Source	Locality
	Unknown
USBM 297	Chester, VT
	Pregratten, Tyrol, Austria
H 116155	Panoche Pass, San Benito Co., CA
S R15127	Calumet Mine, Salida, Chaffee Co. CO
	Catoctin Formation, VT
NIST SRM1867	Fairfax Co. VA
	Unknown
	Mineral Hill, Carroll Co. MD
	Unknown
S 150966	Sebasvatn-Vegardehei, Aust-Agder, Norway
VPI	unknown
	Fair Oaks Commons, Fairfax, VA
S 128320	Near Menzies, Western Australia
S C2530	Aberdeenshire, Scotland
S 5694	Roanoke, VA
H 118781	Copper Mine Hill, Cumberland, Providence Co. RI
S B18698	Maderanertal, Switzerland
S H115199 (= no. 72)	Harvard Museum, RI
	Catoctin Mountain, Frederick County, MD
JM no. 2778-46-5	Mexico
H 115199 (= no. 44)	RI
S C2540-1	Copper Mountain, Prince of Wales Island, AK
S 133524	Newton, CT
	Knappenwand, Sulzbachtal, Salzburg, Austria
	Unknown
	Skyline Drive, VA
	Mineral County, NV
S 118562	St. Gothard Mine, Nevada City, CA
	Cornog, PA
S C2538	Chamounix, Switzerland
S 118989	Amiant, Roselaui, Berner Oberland, Switzerland
S 17881	Cumberland, RI
S 46481	French Creek, Chester County, PA
S 118989	Amiant Rosenhaui Bermer Oberland, Switzerland
	Transvaal, South Africa
	VA?
AMNH 27221	Centerville, VA
USBM 03704	Africa
USBM	South Africa
S 168215	Goose Creek Quarry, Leesburg, Loudon Co. VA
S R3165	Tilly Foster, Brewster, Putnam Co. NY

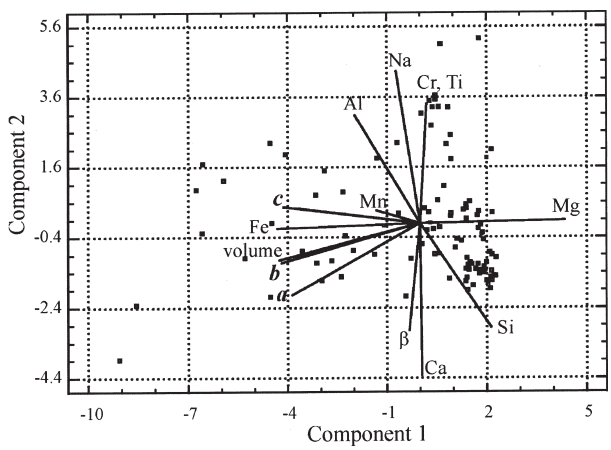

FIGURE 3. Results of principal component analysis with elemental data in apfu. The first two principal components account for 45 and 23% of the total standardized variability in the data, respectively. A smaller data set containing only those samples with measured optical properties was analyzed by using principal component analysis, and the results are not significantly different from those above. All three principal refractive indices load heavily on the first principal component with Fe.

95% prediction limits calculated for our data. Within the limits set by the arbitrary definition of the actinolite series, we find no correlations between composition and unit-cell parameters that can explain the overall deviations from linearity for *a*, *b*, and unit-cell volume. However, none of our samples have ideal compositions, and it is possible that ideal samples would exhibit a linear response in *a*, *b*, and unit-cell volume with respect to ferro-actinolite content. The end-member values are based on regressions of natural samples that have Al > 0, Na > 0, and ^{B}(Fe, Mn, Mg) > 0, on average. The values for end-member ferro-actinolite are extrapolated, and any error in the models for *a*, *b*, and unit-cell volume could have a large effect on the end-member ferro-actinolite values.

There is a correlation between *c* and two minor elements, which is observed as increased scatter about a linear model for samples with greater than 32% ferro-actinolite (Fig. 4c). Principal component analysis of the subset of data for this compositional range indicates a positive correlation of *c* with K and Al. An increase in *c* with tschermakite substitution is demonstrated in studies of synthetic amphiboles on the join tremolite-tschermakite (Smelik et al. 1994; Jenkins et al. 1997). Substitution of K-richterite in tremolite (Hawthorne et al. 1997) produces the opposite response in *c*; however, the average concentration of K in our samples [0.01(2) apfu] is much lower than in any of the synthetic amphiboles. There is also a discrimination in Al (apfu), and by extension the *c* dimension, between asbestiform and non-asbestiform samples. Our data support the earlier conclusion of Dorling and Zussman (1987) that asbestiform actinolite is lower in Al than non-asbestiform actinolite (Fig. 5), although we do not see a similar discrimination in tremolite, and there are too few samples of ferro-actinolite to arrive at a conclusion. Because of the correlation between *c* and Al, we chose to exclude, for the purposes of modeling the behavior in *c* for the series, those samples with Al > 0.3 apfu, which is greater than 1s outside the mean. The complete sample set exhibits the full range in Al allowed under the Leake et al. (1997) definition and so gives an indication of the variation in *c* for the series, although the values predicted by the model are restricted to samples with Al < 0.3 apfu. The samples studied by Evans and Yang (1998) all have Al < 0.3 apfu, and agree well with the linear model for *c*.

The one unit-cell parameter that does not correlate with ferro-actinolite content is β, which instead exhibits a positive correlation with Ca (Fig. 6). This is analogous to the result reported earlier by Evans and Yang (1998), who chose to represent it as a correlation with cummingtonite-grunerite com-

TABLE 2. Microprobe results for standard specimens based on 10 measurements each

Oxide	NIST Glass K411*		Kakanui Hornblende†	
	Measured wt%	Relative error %	Measured wt%	Relative error %
SiO_2	55.0(8)	1.3	40.2(7)	–0.4
FeO	14.5(8)	0.8	10.6(2)	–3.0
MgO	14.9(2)	1.3	12.9(2)	1.1
CaO	15.5(1)	0.4	10.3(1)	0.1
Al_2O_3	–	–	15.1(3)	1.1

* From SRM 470 that also contains glass K412 (Marinenko 1982).
† Measured values of Na_2O, K_2O, and TiO_2 not reported. This sample was used as the standard for these elements.

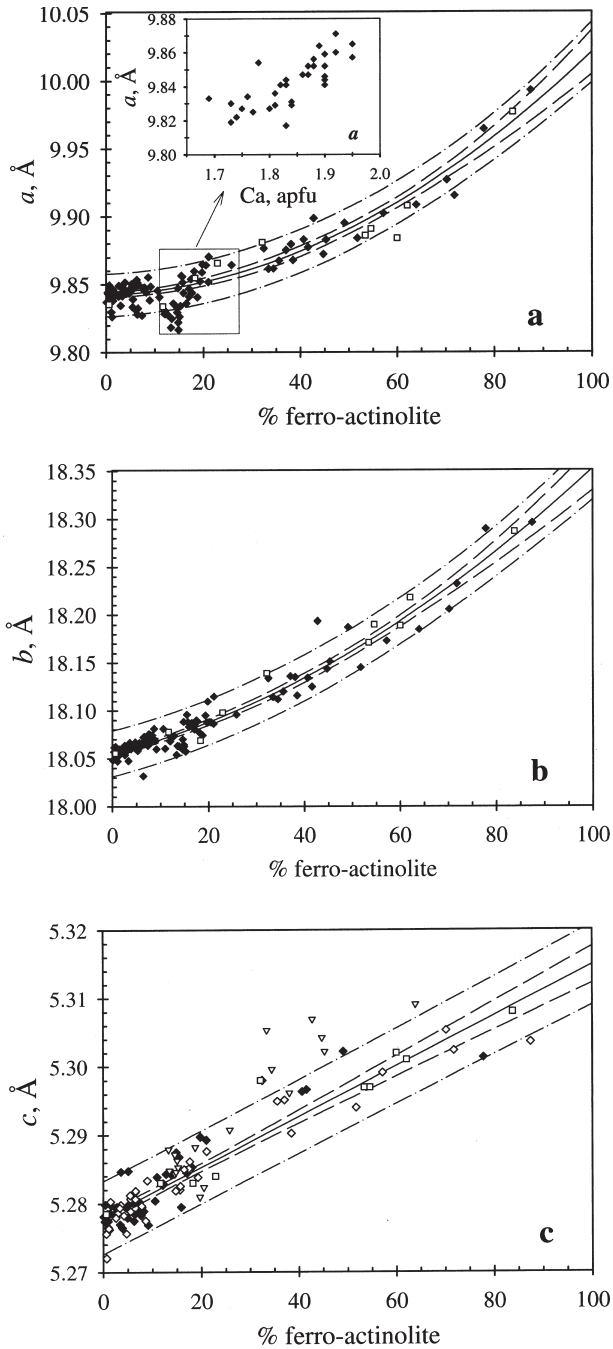

FIGURE 4. Lattice parameters for the actinolite series. Filled diamond, open triangle, open diamond = this work; open box = Evans and Yang (1998). Predicted values from the regressions (solid lines), 95% confidence intervals (dashed lines) and 95% prediction intervals (dashed lines), were calculated by using SigmaPlot. The coefficients of the regressions are: **a**: b(0) = 9.8422 b(1) = 1.58e^{-4}, b(2) = 1.63e^{-5}, R^2 = 0.94, **b**: b(0) = 18.0551, b(1) = 1.31e^{-3}, b(2) = 1.66e^{-5}, R^2 = 0.98, **c**: b(0) = 5.2779, b(1) = 3.7e^{-4}, R^2 = 0.87. Samples with ≥ 0.3 Al apfu (open triangle) were excluded from the regression of *c*. Asbestiform samples (open diamond) are identified in the data for *c*. Values of *a* for compositions between 11 and 26% ferro-actinolite (see inset) were excluded from the regression of *a*.

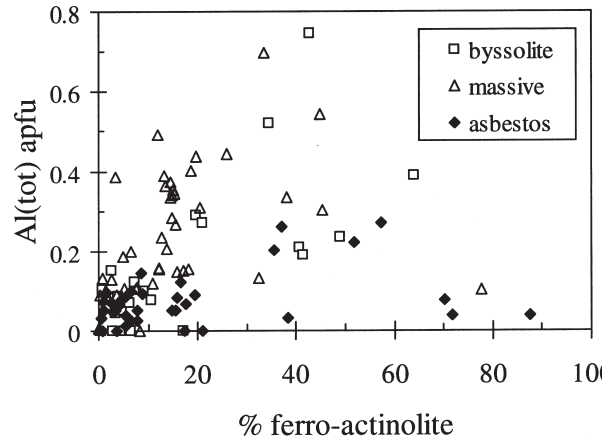

FIGURE 5. Al_{tot} (apfu) distribution in the actinolite series. Mean values of Al_{tot} are 0.06(4) for asbestos and 0.09(8) for massive + "byssolite" for tremolite and 0.09(8) for asbestos and 0.31(16) for massive + "byssolite" for actinolite. Averages for ferro-actinolite not determined.

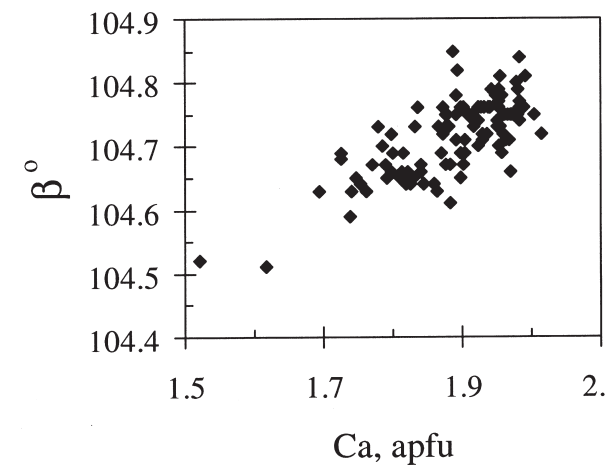

FIGURE 6. Positive correlation of β with Ca, R^2 = 0.54.

ponent. We calculated the index used by Evans and Yang (1998), Ca/(2-^{B}Na), and found no significant difference when using this index in place of Ca. There is also a positive correlation of *a* with Ca, but only for those samples within the range 11–26% ferro-actinolite, which is considered to be an anomalous region for *a*, as described below.

Discontinuity at ~11% ferro-actinolite

There is a break in the data for *a* at approximately 11% ferro-actinolite that is visually compelling (Fig. 4a) and suggestive of a discontinuity. The measurements of *a* for samples with 11–26% ferro-actinolite cannot be modeled with the series by using a simple polynomial model, and for this reason were excluded from the model calculations for *a*. There is a drop in Ca at approximately 11% ferro-actinolite followed by a steady increase in Ca throughout the range 11–26% ferro-actinolite (Fig. 7). There is a positive correlation of *a* with Ca for the range 11–26% ferro-actinolite (Fig. 4a inset), as mentioned previously. The β angle exhibits a similar pattern with a drop at approximately 11% ferro-actinolite (Fig. 8) and then a

steady increase from 11 to 26% ferro-actinolite, consistent with the correlation between Ca and β described previously. There is support from the literature for a drop in Ca at approximately 11% ferro-actinolite, as shown by the general correspondence of the data from Dorling and Zussman (1987), Deer et al. (1997), and Evans and Yang (1998) (Fig. 7). The data from Leake (1968) show more scatter than the other literature data, and there is a sample at 13% ferro-actinolite with Ca = 1.96 apfu. The data in Leake (1968) are bulk analyses and may not refer to single phases.

An additional compositional anomaly for the range 11–26% ferro-actinolite is the presence of relatively high concentrations of Cr and Ti, as compared with the entire series. Our sample set contains 16 Cr- or Ti- bearing samples, and 15 of them have ferro-actinolite contents within the range 11–26% ferro-actinolite. Of the 6 Cr-bearing samples in the collection of Dorling and Zussman (1987), 5 of them are within the range 11–26% ferro-actinolite. The variations in the concentrations of Cr and Ti in our samples are sufficiently marked to represent principal components of variation for the series (Fig. 3), even though the ranges in concentrations for both elements are relatively small (0–0.06 apfu Cr and 0–0.02 apfu Ti). There is also a significant difference in the mean value of Al for samples with 0–10% ferro-actinolite [0.08(7) apfu] as compared with samples with 11–26% ferro-actinolite [0.22(14)] although the ranges in Al are comparable (Fig. 5).

There are also small anomalies in *b* and unit-cell volume at the beginning of the discontinuity (11–16% ferro-actinolite) for which the measured values are systematically smaller than the model values. These samples are predominantly massive and very dark green in color, particularly when compared with the color of massive samples with 5–10% ferro-actinolite (see Table 1).

Optical properties

The principal indices of refraction correlate with ferro-actinolite content, and exhibit no consistent correlations with any other chemical variable. Both n_γ and n_β increase linearly with ferro-actinolite content and show a systematic variation with respect to habit, with the asbestiform samples significantly lower in both indices than the massive and "byssolitic" samples (Figs. 9a and 9b). The variation with respect to habit is consistent with lower Al concentrations for asbestiform actinolites compared with massive and "byssolitic" samples. The orientation of the principal vibration directions with respect to the unit cell (Fig. 10) predicts that *Z* should be most influenced by *c*, whereas *Y* should reflect *b*, and *X* should reflect *a*. The data for n_α cannot be adequately modeled by a single line or with a quadratic equation, which may be indicative of the more complex behavior seen for *a* as opposed to *b* and *c*. The simplest approach to modeling the behavior of n_α is to break the data between 26% and 32% ferro-actinolite, and apply a linear model to each segment. The asbestiform samples appear to have consistently lower values of n_a, but there are insufficient data (due to subdividing the set) to characterize the difference. There is more scatter in n_α than in n_γ, particularly for the compositions below 26% ferro-actinolite. Although fluorine was not measured in this study, it is predicted to lower n_α by as much as 0.01 (Winchell 1963) and part of the variability in n_α may be explained by considering its effect. The residuals from the linear regressions of all 3 principal indices show more scatter in the range 11–26% ferro-actinolite, the same region that was previously identified as anomalous with respect to chemistry and cell parameters.

The end-member values given in Table 4, which are calculated for all the data without respect to habit, are in general agreement with the literature, particularly for n_γ and n_α for the tremolite end-member. Significant discrepancies occur for the ferro-actinolite end-member, and for n_β. The value of 1.700 derived for n_γ for the ferro-actinolite end-member (Deer et al. 1997) from the mean refractive index of synthetic ferro-actinolite (Ernst 1966), agrees with our data, whereas the value of 1.735 (Winchell 1945) predicted from a set of samples whose highest ferro-actinolite content was 51% does not. The values

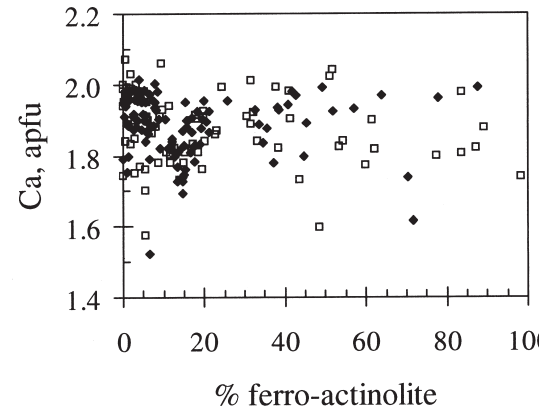

FIGURE 7. Distribution of Ca for the actinolite series. Filled diamond = this work; open box = Dorling and Zussman (1987), Deer et al. (1997), Evans and Yang (1998).

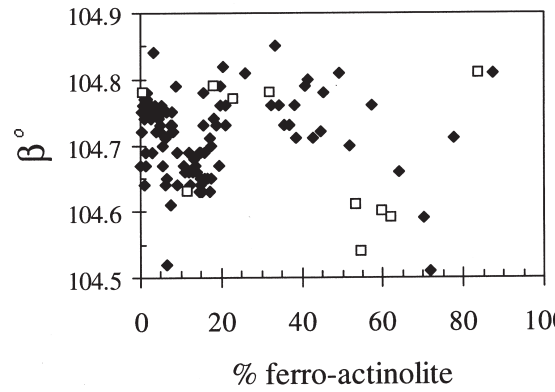

FIGURE 8. Distribution of β for the actinolite series. Filled diamond = this work; open box = Evans and Yang (1998).

TABLE 3. Microprobe results sorted by ferro-actinolite content [(Fe + Mn/Fe + Mn + Mg) = X_{FeA}] with unit formulae calculated on the basis of 23 O

		wt%											
SC	X_{FeA}	SiO_2	TiO_2	Al_2O_3	Cr_2O_3	FeO	MgO	MnO	CaO	Na_2O	K_2O	Total	^{T}Si
216	0.1	59.6	0.0	0.0	0.0	0.0	25.5	0.0	12.5	0.6	0.4	98.6	7.99
193	0.3	58.9	0.0	0.6	0.0	0.1	24.7	0.0	13.2	0.9	0.2	98.6	7.93
249	0.4	59.1	0.0	0.0	0.0	0.2	24.8	0.0	13.5	0.2	0.0	97.8	7.99
48	0.6	58.8	0.0	0.2	0.0	0.2	24.7	0.0	13.7	0.1	0.2	98.0	7.96
29	0.7	57.4	0.0	0.0	0.0	0.2	24.2	0.1	13.0	0.0	0.7	95.7	7.97
213	0.9	57.4	0.0	0.6	0.0	0.3	24.3	0.1	13.4	0.0	0.0	96.3	7.91
240	0.9	57.7	0.0	0.8	0.0	0.4	24.3	0.0	13.5	0.4	0.0	97.2	7.89
239	1.0	58.8	0.0	0.4	0.0	0.4	24.9	0.0	13.0	0.3	0.0	97.8	7.96
247	1.1	56.9	0.0	0.5	0.0	0.1	24.8	0.4	11.8	1.2	0.1	95.8	7.89
231	1.1	59.3	0.0	0.3	0.0	0.4	24.8	0.1	13.7	0.2	0.0	98.8	7.96
194	1.2	59.0	0.0	0.6	0.3	0.1	24.7	0.4	12.5	1.0	0.1	98.6	7.93
250	1.4	58.6	0.0	0.5	0.0	0.1	24.6	0.6	13.0	0.4	0.0	97.7	7.94
144	1.5	58.5	0.0	0.6	0.0	0.6	24.5	0.1	13.4	0.0	0.0	97.8	7.93
128	1.5	59.2	0.0	0.4	0.0	0.5	24.0	0.1	13.5	0.5	0.0	98.3	7.99
61	2.5	58.3	0.0	1.0	0.0	0.9	24.0	0.2	13.3	1.2	0.0	98.9	7.87
9	2.6	58.2	0.0	0.4	0.0	0.9	23.5	0.2	13.5	0.0	0.1	96.9	7.98
198	2.6	57.8	0.0	0.8	0.0	1.1	23.8	0.0	12.8	1.2	0.3	97.8	7.89
31	2.8	58.6	0.0	0.0	0.0	1.0	23.8	0.2	13.0	0.0	0.1	96.7	8.04
226	3.0	57.7	0.0	0.3	0.0	1.2	23.8	0.1	13.3	0.3	0.0	96.6	7.94
147	3.3	55.8	0.0	2.4	0.0	1.4	22.9	0.0	13.3	0.2	0.1	96.2	7.75
185	3.3	59.3	0.0	0.3	0.0	1.4	23.9	0.0	13.0	0.6	0.0	98.8	7.99
138	3.4	57.4	0.0	0.2	0.0	1.4	23.1	0.1	13.1	0.0	0.0	95.3	8.01
37	3.5	57.8	0.0	0.0	0.0	1.4	23.2	0.1	12.7	0.0	0.0	95.3	8.05
146	3.6	56.8	0.0	0.5	0.0	1.5	23.5	0.1	13.1	0.3	0.0	95.8	7.90
15	3.9	57.3	0.0	0.5	0.0	1.6	22.9	0.0	13.6	0.2	0.0	96.2	7.95
254	4.2	56.3	0.0	0.4	0.0	1.3	23.6	0.5	13.1	0.2	0.0	95.4	7.88
8	4.6	57.5	0.0	0.3	0.0	2.0	23.4	0.1	13.2	0.2	0.1	96.8	7.94
248	4.7	58.3	0.0	0.5	0.0	1.9	23.6	0.2	12.8	0.1	0.0	97.5	7.97
204	4.9	57.7	0.0	1.2	0.0	2.0	23.4	0.1	13.2	0.7	0.1	98.5	7.85
30	5.1	56.9	0.0	0.0	0.0	2.1	23.2	0.1	13.2	0.0	0.0	95.6	7.96
184	5.2	58.0	0.0	0.7	0.0	2.2	23.0	0.1	13.0	1.4	0.2	98.4	7.91
238	5.4	57.2	0.0	0.5	0.0	2.1	23.6	0.3	12.4	0.0	0.0	96.1	7.94
242	5.5	56.8	0.0	0.1	0.0	2.2	23.1	0.2	13.0	0.0	0.0	95.4	7.96
155	5.5	57.5	0.0	0.2	0.0	2.3	23.5	0.1	12.9	0.0	0.0	96.7	7.95
229	6.1	58.3	0.0	0.4	0.0	2.4	23.5	0.3	12.7	0.3	0.0	98.1	7.95
47	6.3	58.0	0.0	0.0	0.0	2.6	22.6	0.1	12.7	0.1	0.3	96.5	8.04
199	6.4	57.5	0.0	1.2	0.0	2.7	23.4	0.2	10.4	2.3	0.1	97.8	7.88
52	6.4	57.0	0.0	0.0	0.0	2.4	22.5	0.4	12.4	0.0	0.0	94.7	8.04
14	6.5	57.4	0.0	0.6	0.0	2.7	22.9	0.2	12.0	0.0	0.1	96.0	7.98
140	6.6	56.8	0.0	0.0	0.0	2.6	22.6	0.2	13.1	0.1	0.0	95.5	7.97
49	7.3	57.2	0.0	0.7	0.0	2.9	23.0	0.3	12.7	0.0	0.0	97.0	7.91
245	7.6	58.8	0.0	0.7	0.0	3.2	22.7	0.1	13.5	0.2	0.0	99.2	7.96
232	7.7	58.0	0.0	0.7	0.0	3.0	22.7	0.4	13.3	0.1	0.0	98.0	7.94
214	7.8	57.5	0.0	0.3	0.0	3.3	22.9	0.2	13.1	0.1	0.0	97.4	7.93
143	7.9	57.7	0.0	0.1	0.0	3.1	22.4	0.4	13.5	0.0	0.1	97.3	7.97
43	8.2	56.7	0.0	0.0	0.0	3.3	21.9	0.2	12.7	0.1	0.0	95.0	8.01
46	8.6	57.2	0.0	0.9	0.0	3.3	22.1	0.4	13.4	0.1	0.0	97.5	7.90
154	8.9	57.3	0.0	0.6	0.0	3.5	22.5	0.4	12.9	0.3	0.0	97.4	7.91
148	9.1	57.1	0.0	0.6	0.0	3.6	22.1	0.3	12.2	0.5	0.1	96.6	7.95
208	10.5	57.4	0.0	0.5	0.0	4.4	22.4	0.3	12.9	0.1	0.1	98.0	7.91
202	10.9	57.7	0.0	0.7	0.2	4.4	21.7	0.4	12.4	1.0	0.0	98.6	7.92
157	11.9	55.5	0.1	3.0	0.2	4.9	21.1	0.2	12.3	0.8	0.1	98.3	7.66
224	12.1	56.9	0.0	1.0	0.0	4.8	21.7	0.5	12.4	0.2	0.0	97.5	7.89
206	12.2	56.8	0.0	1.0	0.5	4.9	21.7	0.5	12.5	0.8	0.1	98.6	7.82
210	12.8	56.9	0.0	1.5	0.2	5.3	21.6	0.3	12.2	0.8	0.0	98.8	7.82
205	13.3	55.7	0.1	2.4	0.1	5.4	21.2	0.4	11.6	1.3	0.1	98.3	7.71
187	13.5	56.3	0.1	2.2	0.1	5.6	21.1	0.3	12.0	1.4	0.0	99.0	7.74
246	13.8	55.9	0.0	1.2	0.0	5.3	20.1	0.5	11.9	0.8	0.0	95.7	7.92
156	14.6	56.6	0.0	2.0	0.5	5.9	20.0	0.2	11.4	1.6	0.0	98.2	7.84
160	14.6	56.4	0.1	2.3	0.3	6.2	20.9	0.2	11.7	0.8	0.0	98.9	7.76
129	14.7	57.8	0.0	0.3	0.0	6.1	21.2	0.5	12.7	0.6	0.0	99.2	7.93
192	14.8	56.2	0.0	2.1	0.2	5.9	20.7	0.5	11.7	1.0	0.0	98.5	7.77
45	14.9	56.3	0.0	1.7	0.3	6.1	20.6	0.3	12.3	0.3	0.0	97.8	7.82
207	15.0	56.0	0.1	2.2	0.1	6.0	20.7	0.6	11.8	1.0	0.1	98.6	7.75
203	15.2	56.7	0.1	2.1	0.2	6.0	20.4	0.5	11.9	0.8	0.0	98.8	7.81
25	15.4	56.1	0.0	1.6	0.0	6.1	19.7	0.3	13.0	0.2	0.0	97.0	7.87
139	15.6	55.9	0.0	0.3	0.0	6.3	20.2	0.4	12.3	0.4	0.0	95.8	7.96
253	15.7	55.6	0.0	0.5	0.0	6.5	20.3	0.3	12.4	0.1	0.0	95.7	7.92
141	15.9	55.9	0.0	0.9	0.0	6.2	20.0	0.5	12.6	0.7	0.0	96.8	7.89
188	16.5	55.3	0.0	0.7	0.0	6.6	20.4	0.6	11.8	0.1	0.1	95.6	7.90
153	17.0	55.5	0.0	0.9	0.1	6.7	19.8	0.6	12.5	0.1	0.0	96.1	7.89
161	17.0	57.7	0.0	0.0	0.0	7.4	20.4	0.1	12.6	0.9	0.0	99.0	7.97

Note: Average values for some of the columns are as follows: ^{T}Si = 7.88(.11), ^{T}Al = 0.10(11), ^{C}Al = 0.06(6), Cr = 0.01(1), Ti = 0.00(0), ΣC = 5.09(7), Ca = 1.89(9), ^{B}Na = 0.04(5), ^{A}Na = 0.09(9), ^{A}K = 0.01(2).

TABLE 3—*Extended*

^{T}Al	Σ T	^{C}Al	Mg	Cr	Ti	Fe	Mn	Σ C	Ca	^{B}Na	Σ B	^{A}Na	^{A}K	Σ A
0.01	8.00	0.00	5.09	0.00	0.00	0.01	0.00	5.10	1.79	0.11	2.00	0.04	0.07	0.11
0.07	8.00	0.02	4.95	0.00	0.00	0.01	0.00	4.99	1.91	0.09	2.00	0.14	0.04	0.17
0.00	7.99	0.00	5.01	0.00	0.00	0.02	0.00	5.03	1.96	0.01	2.00	0.05	0.00	0.05
0.00	7.96	0.03	4.99	0.00	0.00	0.03	0.01	5.05	1.98	0.00	2.03	0.02	0.03	0.05
0.00	7.97	0.00	5.01	0.00	0.00	0.03	0.01	5.05	1.94	0.00	1.99	0.01	0.12	0.12
0.09	8.00	0.01	5.00	0.00	0.00	0.04	0.01	5.05	1.98	0.00	2.04	0.01	0.00	0.01
0.11	8.00	0.02	4.94	0.00	0.00	0.05	0.00	5.01	1.98	0.01	2.00	0.10	0.00	0.10
0.04	8.00	0.02	5.02	0.00	0.00	0.05	0.00	5.09	1.89	0.02	2.00	0.04	0.00	0.04
0.00	7.89	0.08	5.12	0.00	0.00	0.01	0.04	5.26	1.75	0.00	2.01	0.33	0.02	0.35
0.04	8.00	0.01	4.95	0.00	0.00	0.04	0.02	5.02	1.97	0.01	2.00	0.05	0.00	0.05
0.07	8.00	0.03	4.94	0.03	0.00	0.02	0.05	5.07	1.80	0.14	2.00	0.13	0.01	0.14
0.06	8.00	0.03	4.98	0.00	0.00	0.01	0.07	5.08	1.88	0.04	2.00	0.07	0.00	0.07
0.07	8.00	0.03	4.96	0.00	0.00	0.07	0.01	5.07	1.95	0.00	2.02	0.00	0.00	0.00
0.01	8.00	0.05	4.83	0.00	0.00	0.06	0.01	4.96	1.96	0.04	2.00	0.08	0.00	0.08
0.13	8.00	0.02	4.83	0.00	0.00	0.11	0.02	4.98	1.92	0.08	2.00	0.24	0.00	0.24
0.02	8.00	0.05	4.81	0.00	0.00	0.11	0.02	4.99	1.99	0.00	1.99	0.00	0.01	0.01
0.11	8.00	0.02	4.84	0.00	0.00	0.13	0.00	4.99	1.87	0.13	2.00	0.18	0.05	0.24
0.00	8.04	0.00	4.86	0.00	0.00	0.12	0.02	5.01	1.91	0.00	1.92	0.00	0.02	0.02
0.00	7.94	0.05	4.90	0.00	0.00	0.13	0.02	5.10	1.96	0.00	2.05	0.07	0.00	0.07
0.25	8.00	0.13	4.73	0.00	0.00	0.16	0.01	5.03	1.98	0.00	2.02	0.06	0.02	0.08
0.01	8.00	0.04	4.80	0.00	0.00	0.16	0.00	5.02	1.88	0.10	2.00	0.06	0.00	0.06
0.00	8.01	0.03	4.80	0.00	0.00	0.16	0.01	5.01	1.96	0.00	1.97	0.00	0.00	0.00
0.00	8.05	0.00	4.82	0.00	0.00	0.16	0.01	5.00	1.90	0.00	1.90	0.00	0.01	0.01
0.00	7.90	0.09	4.88	0.00	0.00	0.17	0.01	5.15	1.95	0.00	2.11	0.08	0.00	0.08
0.05	8.00	0.04	4.73	0.00	0.00	0.19	0.00	4.96	2.02	0.00	2.02	0.04	0.01	0.05
0.00	7.88	0.07	4.93	0.00	0.00	0.16	0.06	5.21	1.97	0.00	2.18	0.05	0.00	0.05
0.00	7.94	0.05	4.81	0.00	0.00	0.23	0.01	5.10	1.95	0.00	2.05	0.06	0.02	0.08
0.03	8.00	0.05	4.81	0.00	0.00	0.21	0.02	5.10	1.87	0.03	2.00	0.01	0.00	0.01
0.15	8.00	0.03	4.75	0.00	0.00	0.23	0.01	5.03	1.92	0.05	2.00	0.15	0.01	0.16
0.00	7.96	0.00	4.84	0.00	0.00	0.24	0.02	5.10	1.98	0.00	2.08	0.00	0.00	0.00
0.09	8.00	0.01	4.67	0.00	0.00	0.25	0.01	4.94	1.90	0.10	2.00	0.26	0.03	0.29
0.06	8.00	0.02	4.88	0.00	0.00	0.25	0.03	5.18	1.84	0.00	2.02	0.00	0.00	0.00
0.00	7.96	0.01	4.82	0.00	0.00	0.26	0.02	5.12	1.95	0.00	2.07	0.00	0.00	0.00
0.00	7.95	0.04	4.83	0.00	0.00	0.27	0.02	5.16	1.91	0.00	2.07	0.00	0.00	0.00
0.05	8.00	0.02	4.78	0.00	0.00	0.28	0.04	5.12	1.86	0.02	2.00	0.05	0.00	0.05
0.00	8.04	0.00	4.68	0.00	0.00	0.30	0.02	4.99	1.89	0.00	1.89	0.04	0.05	0.09
0.12	8.00	0.08	4.78	0.00	0.00	0.31	0.02	5.18	1.52	0.29	2.00	0.32	0.02	0.34
0.00	8.04	0.00	4.72	0.00	0.00	0.28	0.05	5.05	1.88	0.00	1.92	0.00	0.00	0.00
0.02	8.00	0.08	4.74	0.00	0.00	0.31	0.02	5.16	1.79	0.00	1.95	0.00	0.02	0.02
0.00	7.97	0.01	4.72	0.00	0.00	0.30	0.03	5.06	1.97	0.00	2.03	0.04	0.00	0.04
0.09	8.00	0.03	4.73	0.00	0.00	0.34	0.04	5.14	1.88	0.00	2.03	0.00	0.00	0.00
0.04	8.00	0.06	4.58	0.00	0.00	0.36	0.01	5.01	1.95	0.03	2.00	0.01	0.00	0.01
0.06	8.00	0.04	4.63	0.00	0.00	0.34	0.04	5.05	1.95	0.00	2.00	0.01	0.00	0.01
0.00	7.93	0.05	4.72	0.00	0.00	0.38	0.02	5.17	1.94	0.00	2.11	0.02	0.01	0.03
0.00	7.97	0.02	4.62	0.00	0.00	0.35	0.04	5.04	2.00	0.00	2.04	0.00	0.01	0.01
0.00	8.01	0.00	4.61	0.00	0.00	0.39	0.03	5.03	1.93	0.00	1.96	0.02	0.01	0.02
0.10	8.00	0.05	4.56	0.00	0.00	0.38	0.05	5.03	1.98	0.00	2.02	0.01	0.01	0.02
0.09	8.00	0.01	4.63	0.00	0.00	0.41	0.05	5.10	1.90	0.00	2.00	0.08	0.00	0.08
0.05	8.00	0.05	4.59	0.00	0.00	0.42	0.04	5.10	1.82	0.08	2.00	0.05	0.02	0.07
0.00	7.91	0.08	4.60	0.00	0.00	0.50	0.04	5.22	1.90	0.00	2.12	0.02	0.01	0.03
0.08	8.00	0.04	4.44	0.02	0.00	0.50	0.04	5.05	1.82	0.13	2.00	0.15	0.00	0.15
0.34	8.00	0.16	4.35	0.03	0.01	0.56	0.03	5.13	1.81	0.05	2.00	0.16	0.02	0.18
0.11	8.00	0.05	4.50	0.00	0.00	0.56	0.06	5.16	1.84	0.00	2.00	0.06	0.00	0.06
0.00	7.82	0.16	4.45	0.05	0.00	0.56	0.06	5.28	1.84	0.00	2.13	0.22	0.01	0.23
0.18	8.00	0.06	4.42	0.02	0.00	0.61	0.03	5.14	1.80	0.06	2.00	0.16	0.00	0.17
0.29	8.00	0.10	4.37	0.01	0.01	0.63	0.04	5.16	1.73	0.11	2.00	0.24	0.02	0.27
0.26	8.00	0.10	4.32	0.01	0.01	0.64	0.03	5.11	1.77	0.12	2.00	0.26	0.00	0.26
0.08	8.00	0.12	4.26	0.00	0.00	0.63	0.05	5.06	1.81	0.13	2.00	0.09	0.00	0.09
0.16	8.00	0.17	4.13	0.05	0.00	0.68	0.03	5.06	1.69	0.25	2.00	0.18	0.01	0.19
0.24	8.00	0.13	4.29	0.03	0.01	0.71	0.02	5.19	1.73	0.08	2.00	0.14	0.00	0.14
0.00	7.93	0.05	4.35	0.00	0.00	0.70	0.05	5.16	1.87	0.00	2.03	0.15	0.00	0.16
0.23	8.00	0.12	4.28	0.02	0.00	0.68	0.06	5.16	1.74	0.10	2.00	0.18	0.00	0.18
0.18	8.00	0.11	4.26	0.03	0.00	0.71	0.03	5.15	1.83	0.03	2.00	0.06	0.00	0.06
0.25	8.00	0.10	4.28	0.01	0.01	0.69	0.07	5.16	1.75	0.09	2.00	0.19	0.02	0.21
0.19	8.00	0.16	4.19	0.02	0.01	0.69	0.06	5.12	1.76	0.11	2.00	0.11	0.00	0.11
0.13	8.00	0.14	4.12	0.00	0.00	0.71	0.04	5.02	1.95	0.03	2.00	0.02	0.01	0.02
0.00	7.96	0.04	4.29	0.00	0.00	0.75	0.05	5.13	1.88	0.00	2.01	0.11	0.00	0.11
0.08	8.00	0.01	4.32	0.00	0.00	0.77	0.03	5.13	1.90	0.00	2.02	0.02	0.00	0.02
0.11	8.00	0.03	4.20	0.00	0.00	0.73	0.06	5.04	1.90	0.06	2.00	0.13	0.00	0.13
0.10	8.00	0.02	4.33	0.00	0.00	0.78	0.07	5.21	1.81	0.00	2.02	0.04	0.01	0.05
0.11	8.00	0.04	4.20	0.01	0.00	0.79	0.07	5.12	1.90	0.00	2.02	0.01	0.00	0.02
0.00	7.97	0.00	4.21	0.00	0.00	0.85	0.01	5.07	1.86	0.06	2.00	0.17	0.00	0.17

—Continued next page

TABLE 3—*Continued*

		wt%											
SC	X_{FeA}	SiO_2	TiO_2	Al_2O_3	Cr_2O_3	FeO	MgO	MnO	CaO	Na_2O	K_2O	Total	^{T}Si
255	17.4	53.9	0.0	0.0	0.0	7.0	19.4	0.3	11.2	0.6	0.1	92.4	7.98
137	17.6	56.0	0.0	0.5	0.0	7.2	20.0	0.5	12.0	0.4	0.0	96.5	7.94
158	18.1	55.9	0.0	0.9	0.1	7.6	19.6	0.1	12.8	0.9	0.0	98.0	7.85
163	18.7	55.5	0.0	2.4	0.1	7.4	19.3	0.5	12.3	1.0	0.1	98.7	7.73
7	19.3	56.5	0.0	0.5	0.0	7.9	19.7	0.5	12.5	0.1	0.1	97.7	7.93
200	19.7	54.5	0.0	2.6	0.0	7.8	19.0	0.5	12.7	1.3	0.3	98.8	7.64
110	19.8	54.2	0.0	1.7	0.0	7.6	18.6	0.6	12.7	0.2	0.1	95.6	7.80
44	20.5	54.6	0.0	1.8	0.0	7.8	18.4	0.7	12.4	0.6	0.3	96.5	7.80
151	21.0	55.0	0.0	1.6	0.0	8.4	18.8	0.5	12.3	0.3	0.1	96.9	7.82
227	21.1	57.6	0.0	0.0	0.0	8.8	19.4	0.4	12.9	0.1	0.0	99.2	7.99
72	25.8	51.7	0.0	2.6	0.0	10.0	17.2	0.6	12.4	0.7	0.3	95.6	7.58
26	32.5	55.2	0.0	0.8	0.0	13.2	16.1	0.6	12.6	0.0	0.0	98.6	7.89
159	33.4	52.7	0.0	4.1	0.0	12.5	15.0	0.9	12.3	1.0	0.1	98.7	7.55
12	34.4	52.5	0.0	3.0	0.0	13.4	14.8	0.4	11.7	0.8	0.2	96.8	7.68
235	35.6	54.5	0.0	1.2	0.0	13.9	14.9	0.7	12.1	0.5	0.0	97.8	7.89
150	37.1	51.4	0.0	1.4	0.0	13.7	14.0	0.9	10.9	0.8	0.1	93.2	7.83
225	38.1	53.8	0.0	1.9	0.0	14.8	13.9	0.4	12.4	0.1	0.0	97.3	7.84
38	38.5	55.0	0.0	0.2	0.0	14.9	14.2	0.9	12.4	0.7	0.0	98.5	7.96
201	40.7	54.5	0.0	1.2	0.0	15.6	13.3	0.8	12.5	0.6	0.1	98.6	7.89
60	41.5	54.0	0.0	1.1	0.0	16.5	13.5	0.6	12.7	0.1	0.2	98.7	7.85
54	42.7	51.4	0.0	4.3	0.0	16.1	12.5	0.6	12.6	0.6	0.2	98.4	7.52
162	44.7	52.0	0.0	3.2	0.0	17.7	12.6	0.6	11.5	1.0	0.2	98.8	7.61
20	45.3	53.0	0.0	1.7	0.0	17.8	12.2	0.3	11.9	0.3	0.1	97.4	7.84
109	49.1	52.9	0.0	1.3	0.0	18.8	11.3	0.6	12.5	0.1	0.1	97.7	7.86
132	51.7	52.6	0.0	1.3	0.0	19.8	11.1	1.5	12.1	0.5	0.1	99.0	7.79
149	57.1	52.3	0.0	1.5	0.0	22.2	9.7	1.0	12.1	0.1	0.2	99.2	7.79
107	63.9	50.5	0.0	2.2	0.0	24.5	8.1	1.0	12.1	0.2	0.1	98.6	7.67
66	70.2	49.6	0.0	0.4	0.0	26.4	6.5	1.0	10.2	1.0	0.2	95.3	7.89
115	71.8	52.0	0.0	0.2	0.0	27.8	6.4	1.1	9.8	1.2	0.1	98.6	7.98
164	77.8	50.8	0.0	0.6	0.0	28.3	4.7	1.3	11.8	0.5	0.0	98.0	7.91
94	87.5	49.7	0.0	0.2	0.0	32.9	2.7	0.7	11.7	0.2	0.2	98.2	7.90

Note: Average values for some of the columns are as follows: ^{T}Si = 7.88(.11), ^{T}Al = 0.10(11), ^{C}Al = 0.06(6), Cr = 0.01(1), Ti = 0.00(0), ΣC = 5.09(7), Ca = 1.89(9), ^{B}Na = 0.04(5), ^{A}Na = 0.09(9), ^{A}K = 0.01(2).

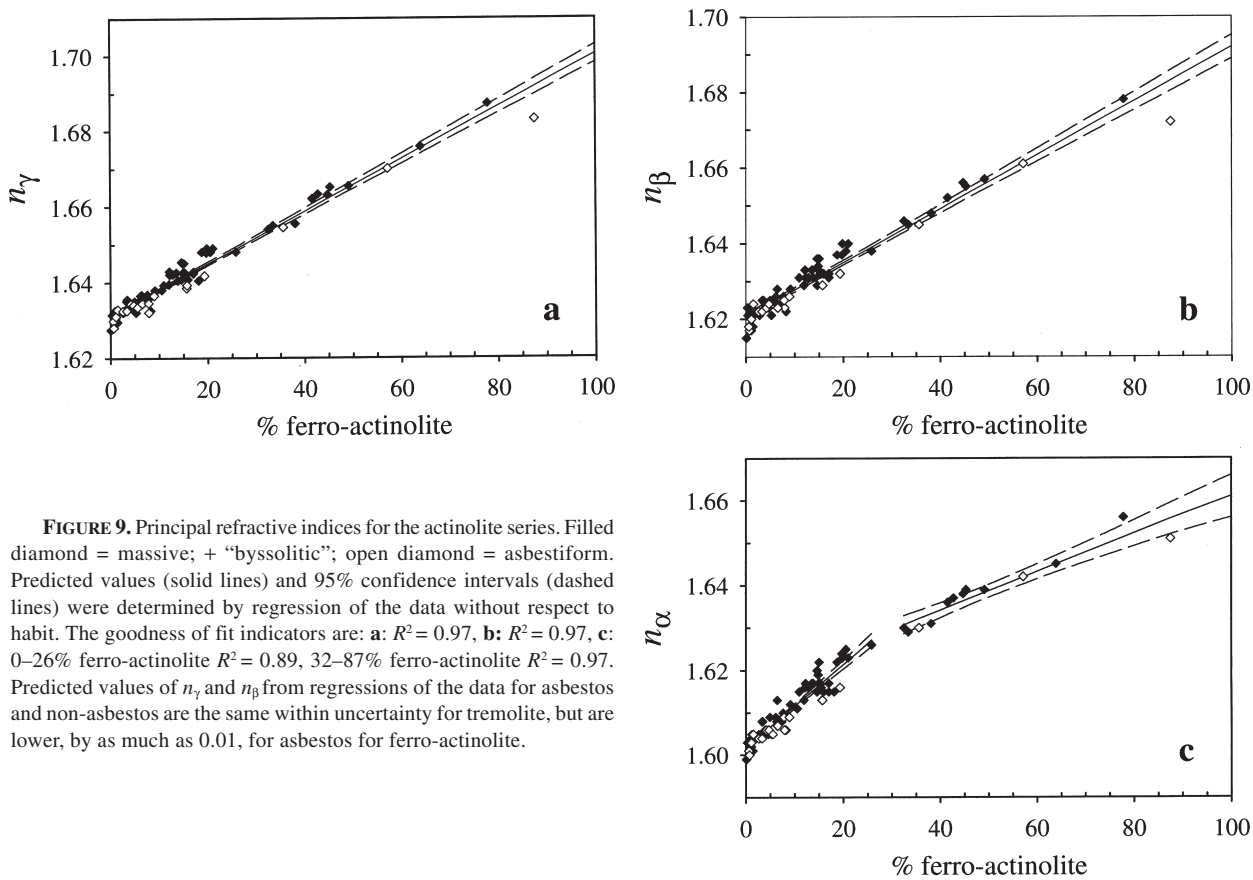

FIGURE 9. Principal refractive indices for the actinolite series. Filled diamond = massive; + "byssolitic"; open diamond = asbestiform. Predicted values (solid lines) and 95% confidence intervals (dashed lines) were determined by regression of the data without respect to habit. The goodness of fit indicators are: **a**: $R^2 = 0.97$, **b:** $R^2 = 0.97$, **c**: 0–26% ferro-actinolite $R^2 = 0.89$, 32–87% ferro-actinolite $R^2 = 0.97$. Predicted values of n_γ and n_β from regressions of the data for asbestos and non-asbestos are the same within uncertainty for tremolite, but are lower, by as much as 0.01, for asbestos for ferro-actinolite.

TABLE 3—*Extended*

^{T}Al	Σ T	^{C}Al	Mg	Cr	Ti	Fe	Mn	Σ C	Ca	^{B}Na	Σ B	^{A}Na	^{A}K	Σ A
0.00	7.98	0.00	4.27	0.00	0.00	0.87	0.03	5.17	1.78	0.04	2.00	0.12	0.01	0.13
0.06	8.00	0.02	4.22	0.00	0.00	0.85	0.05	5.14	1.83	0.03	2.00	0.08	0.00	0.08
0.15	8.00	0.00	4.09	0.01	0.00	0.89	0.02	5.02	1.92	0.06	2.00	0.19	0.00	0.19
0.27	8.00	0.13	4.01	0.01	0.00	0.86	0.06	5.08	1.83	0.09	2.00	0.19	0.02	0.21
0.07	8.00	0.02	4.12	0.00	0.00	0.92	0.06	5.13	1.88	0.00	2.00	0.02	0.01	0.03
0.36	8.00	0.08	3.98	0.00	0.00	0.91	0.06	5.03	1.90	0.06	2.00	0.28	0.06	0.34
0.20	8.00	0.09	3.98	0.00	0.00	0.91	0.07	5.06	1.95	0.00	2.01	0.07	0.02	0.09
0.20	8.00	0.11	3.92	0.00	0.00	0.93	0.08	5.04	1.89	0.06	2.00	0.11	0.05	0.16
0.18	8.00	0.09	3.98	0.00	0.00	1.00	0.06	5.13	1.87	0.00	2.00	0.08	0.01	0.10
0.00	7.99	0.00	4.01	0.00	0.00	1.02	0.05	5.08	1.92	0.00	2.00	0.02	0.00	0.02
0.42	8.00	0.02	3.77	0.00	0.00	1.23	0.08	5.11	1.95	0.00	2.07	0.20	0.05	0.25
0.11	8.00	0.02	3.43	0.00	0.00	1.58	0.08	5.11	1.93	0.00	2.04	0.00	0.00	0.01
0.45	8.00	0.25	3.20	0.00	0.00	1.49	0.11	5.06	1.89	0.05	2.00	0.23	0.01	0.25
0.32	8.00	0.19	3.22	0.00	0.00	1.64	0.05	5.10	1.84	0.06	2.00	0.16	0.03	0.19
0.11	8.00	0.09	3.21	0.00	0.00	1.68	0.09	5.06	1.88	0.06	2.00	0.09	0.00	0.09
0.17	8.00	0.09	3.17	0.00	0.00	1.75	0.12	5.14	1.78	0.09	2.00	0.14	0.02	0.16
0.16	8.00	0.18	3.01	0.00	0.00	1.81	0.05	5.04	1.94	0.02	2.00	0.00	0.00	0.00
0.00	7.96	0.03	3.07	0.00	0.00	1.81	0.11	5.03	1.93	0.04	2.00	0.15	0.01	0.15
0.11	8.00	0.10	2.88	0.00	0.00	1.89	0.09	4.97	1.94	0.06	2.00	0.12	0.01	0.13
0.15	8.00	0.04	2.93	0.00	0.00	2.00	0.08	5.05	1.98	0.00	2.03	0.03	0.03	0.06
0.48	8.00	0.26	2.73	0.00	0.00	1.97	0.07	5.04	1.97	0.00	2.00	0.17	0.04	0.21
0.39	8.00	0.15	2.76	0.00	0.00	2.16	0.07	5.15	1.80	0.05	2.00	0.23	0.04	0.28
0.16	8.00	0.14	2.70	0.00	0.00	2.20	0.03	5.06	1.89	0.04	2.00	0.04	0.02	0.07
0.14	8.00	0.10	2.50	0.00	0.00	2.33	0.08	5.00	1.99	0.00	2.00	0.02	0.02	0.04
0.21	8.00	0.01	2.45	0.00	0.00	2.45	0.18	5.10	1.92	0.00	2.02	0.13	0.02	0.15
0.21	8.00	0.05	2.16	0.00	0.00	2.76	0.12	5.11	1.93	0.00	2.04	0.03	0.04	0.07
0.33	8.00	0.06	1.83	0.00	0.00	3.11	0.13	5.13	1.97	0.00	2.10	0.05	0.02	0.07
0.00	7.89	0.08	1.54	0.00	0.00	3.51	0.13	5.26	1.74	0.00	2.00	0.31	0.04	0.35
0.02	8.00	0.02	1.46	0.00	0.00	3.57	0.14	5.19	1.62	0.19	2.00	0.16	0.03	0.19
0.09	8.00	0.02	1.10	0.00	0.00	3.69	0.17	4.99	1.96	0.04	2.00	0.12	0.01	0.13
0.00	7.90	0.04	0.64	0.00	0.00	4.37	0.09	5.14	1.99	0.00	2.13	0.06	0.04	0.09

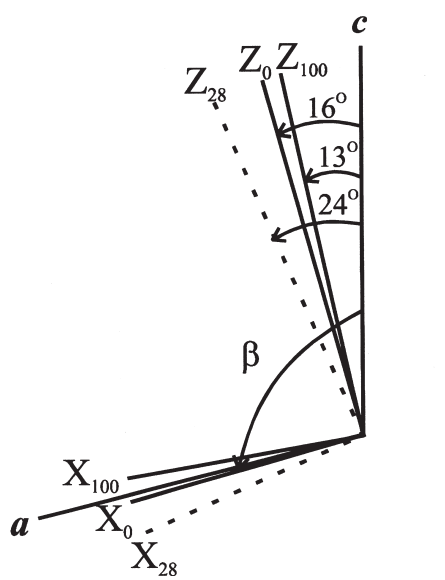

FIGURE 10. Schematic representation of the orientations of principal vibration directions Z (n_γ) and X (n_α) with respect to (010) for 3 different ferro-actinolite concentrations. Extinction angles ($c \wedge Z$) are representative of the data for Z_0 and Z_{100}. The extinction angle given by the dotted line for Z_{28} is taken from Deer et al. (1997) and indicates a possible maximum value for the compositional region 20 to 32% ferro-actinolite. Principal vibration direction Y (n_β) is parallel to b.

given for n_α for the ferro-actinolite end-member are 1.680 (Deer et al. 1997) for synthetic ferro-actinolite (which has significant grunerite in solid solution), and 1.6717 (Winchell 1963), both of which are significantly higher than our value. Values of n_α higher than our value of 1.661 would be obtained for the ferro-actinolite end-member by using a single linear regression applied throughout the series, an approach not supported by the data in this study. The single value given in the literature for n_β for the tremolite end-member is 1.6146 (Winchell 1963), which is significantly lower than our data would predict. The value of n_β given by Winchell (1963) for the ferro-actinolite end member is 1.6856 whereas Ernst (1966) reports a value of 1.689(3), which is within the uncertainty of our predicted value.

TABLE 4. Predicted end-member values

	Tremolite	Ferro-actinolite
a	9.841 ± 0.003 Å	10.021 ± 0.011 Å
b	18.055 ± 0.004 Å	18.353 ± 0.018 Å
c	5.278 ± 0.001 Å	5.315 ± 0.003 Å
V	906.6 ± 0.5 Å^3	944 ± 2 Å^3
n_α	1.602 ± 0.001	1.661 ± 0.005
n_β	1.621 ± 0.001	1.692 ± 0.004
n_γ	1.631 ± 0.001	1.700 ± 0.003

Notes: Predicted values for the end-members are derived from the regression of the data. The uncertainties are calculated as 95% confidence limits on the regression and are approximate expanded uncertainties with a coverage factor k = 2. The predicted values and uncertainties for the ferro-actinolite end-member are extrapolated, as the data do not extend past 87% ferro-actinolite. End-member values were calculated for *a* after exclusion of the data from 11–26% ferro-actinolite. End-member values were calculated for *c* after exclusion of the data containing ≥0.3 Al apfu. Cell volumes calculated from model values of *a*, *b*, *c*, and β-angles of 104.72° (tremolite) and 104.81° (ferro-actinolite) are 907.0 Å^3 and 945.0 Å^3 respectively, which are within the uncertainties of the predicted values.

It has been generally assumed that birefringence (n_γ–n_α) decreases with ferro-actinolite content (Phillips and Griffen 1981; Nesse 1991; Deer et al. 1997), although it is clear from the behavior of n_α that there is not a simple relationship between birefringence and ferro-actinolite content. Accordingly, our measurements of birefringence are best modeled by considering two populations, as for n_α, with a linear decrease from 0 to 26% ferro-actinolite, and a linear increase from 32 to 100% ferro-actinolite (Fig. 11a). The linear models can be calculated as the difference between the linear regressions of n_α and n_γ, or by linear regressions of the calculated birefringence for each sample. The end-member values determined by using the two approaches are slightly different, but agree within the uncertainties associated with each approach.

The data for extinction angle (Fig. 11b) could support the conclusion in the literature that extinction angle decreases with ferro-actinolite content, although a linear regression of the data indicates a very poor fit (R^2 = 0.27). Similar to the data reported by Deer et al. (1997), our highest extinction angles occur from 20 to 30% ferro-actinolite. An alternative hypothesis, supported by the patterns observed in n_α and birefringence, is to consider two populations of extinction angles, one between 0 and 26% ferro-actinolite and a second between 32 and 87% ferro-actinolite. The first population is best described by an average value of 16.3(0.8)° with outliers (> 2s) at 14.8, 19.7, 20.5, and 25.8% ferro-actinolite, and the second by a linear decrease from 15.1 to 13.2°, although the fit is still poor (R^2 = 0.43).

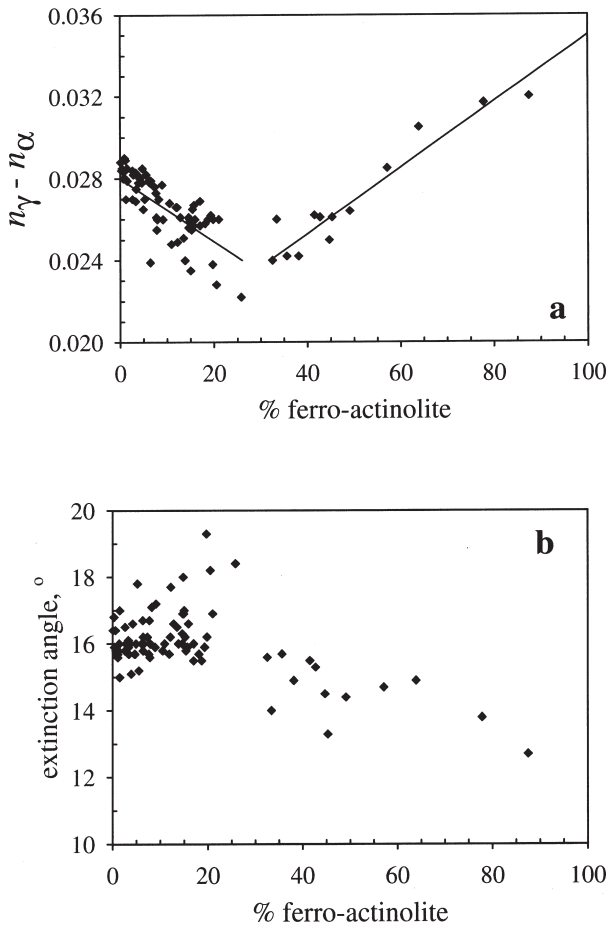

FIGURE 11. Distribution of (**a**) birefringence (n_γ–n_α) and (**b**) extinction angle for the actinolite series. Linear regressions of birefringence with respect to ferro-actinolite content are given by solid lines (R^2 = 0.62 for 0–26% ferro-actinolite, and R^2 = 0.91 for 32–87% ferro-actinolite).

Discontinuity between 26 and 32% ferro-actinolite

The discontinuity between 26 and 32% ferro-actinolite indicated by n_α, birefringence, and extinction angle is not accompanied by any clearly defined change in lattice dimensions or chemistry. Evans and Medenbach (1997) reported a change in optical properties (extinction angle and optic axial angle) for cummingtonite at $X_{Fe} \approx 0.3$ that they attributed to M-site ordering of Mg and Fe. Site preferences for Mg and Fe in the actinolite series are very small (Evans and Yang 1998), and therefore cannot explain the discontinuity between 26 and 32% ferro-actinolite. We provide evidence that Al may play a role in the discontinuity. The positive correlation between *c* and Al is observed only for samples with greater than 32% ferro-actinolite, even though there is almost as large a range in Al, considering either Al_{tot} or ^{C}Al (Fig. 12) for samples with 0–26% ferro-actinolite. The residuals from the linear regression of Fe + Mn vs. Mg (Fig. 1) are not random above 32% ferro-actinolite, but instead are generally negative (Fe + Mn + Mg < 5 apfu) for 32 to 50% ferro-actinolite, and generally positive for 50 to 87% ferro-actinolite. The residuals indicate excess tschermakite component from 32 to 50% ferro-actinolite, and excess cummingtonite-grunerite component from 50 to 87% ferro-actinolite.

The distribution of Al (apfu) with ferro-actinolite content is in general agreement with the positive correlation of Al and Fe

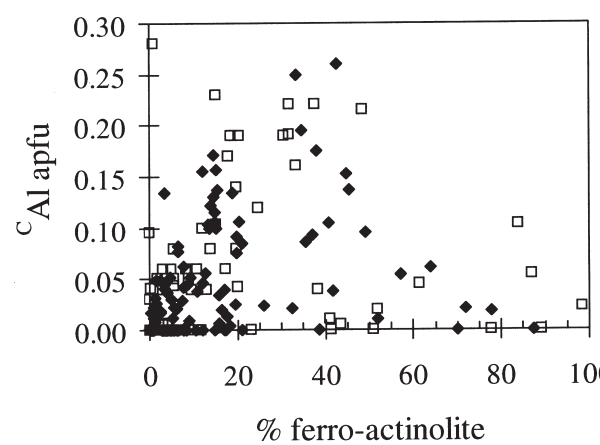

FIGURE 12. The distribution of ^{C}Al (apfu) for the actinolite series. Filled diamond = this work; open box = Dorling and Zussman (1987), Deer et al. (1997).

in calcic amphiboles (Léger and Ferry 1991). However, ferro-actinolite is lower in Al (particularly ^{C}Al) than actinolite, and, in our data, similar to tremolite. This could be a consequence of variables not tested for in this study, specifically the pressure and temperature of formation, bulk rock composition, and coexisting mineral assemblage (Léger and Ferry 1991). Ferro-actinolites are commonly found in metamorphosed iron formations (Robinson et al. 1982; Deer et al. 1997), and the low Al content of these ferro-actinolites may be a function of the low Al contents of the host rocks (Robinson et al. 1982). Ferro-actinolites are rare in comparison with tremolite and actinolite, and therefore compositional data are scarce, both in our work and in the literature. The Al distribution for samples from Dorling and Zussman (1987) and Deer et al. (1997) is consistent with our data (Fig. 12). If the Al distribution does peak between 30 and 50% ferro-actinolite, we can speculate that the solid solution with hornblende exists only for this compositional range. A limited solid solution for other portions of the actinolite series may be the cause of the discontinuity observed in the optical properties. The possibility of a miscibility gap between actinolite and hornblende has been widely debated, with evidence presented for both sides (for a review see Robinson et al. 1982).

Our sample collection happens to have no representatives between 26 and 32% ferro-actinolite, which prevents us from ascertaining, any closer, the position of the discontinuity. The sample reported by Deer et al. (1997) at 28% ferro-actinolite has an extinction angle of 24°, which implies that it belongs with the population of samples with ferro-actinolite contents on the low side of the discontinuity. A histogram of ferro-actinolite content, based on our data (103 samples) combined with 137 samples compiled from the literature (Dorling and Zussman 1987; Evans and Yang 1998; Deer et al. 1997; and Leake 1968) suggests that samples with ferro-actinolite contents from 26 to 32% are relatively uncommon when compared with nearby compositions (Fig. 13). The relative frequency of samples is generally low throughout the range 30–100% and the apparent gap at ~28% may simply reflect inadequate sampling. It is interesting, however, that there is a drop in frequency at 10–12% ferro-actinolite, which is the location of the discontinuity observed in *a* and which is characterized by a drop in Ca concentration, as described previously.

SUMMARY REMARKS

It has long been assumed that the complexity of amphiboles would make difficult, or impossible, the determination of systematic relationships by the study of natural specimens (e.g., Ernst 1968). While there is no doubt that the studies of synthetic amphiboles have added greatly to the understanding of amphibole systematics, it is difficult to model all relevant variables, as is clear from the discrepancies between synthetic and natural tremolite. We hope this report has demonstrated the information that can be discerned from the study of many natural specimens that may not be available in any other manner. It was critical to the conclusions in this study that all the data were collected and processed under the same conditions such that the uncertainties could be evaluated, which is not possible for studies based on measurements compiled from the literature. The personal computing power available today coupled with the sophisticated programs available for use in microprobe analysis, powder diffraction, and general data analysis, and the automation of much of the data collection for chemical and crystallographic analyses, have made possible the type of study reported here.

In the nomenclature of amphiboles the subdivisions of tremolite, actinolite, and ferro-actinolite were retained "*because of the strong desire especially, but not solely, expressed by metamorphic petrologists to retain the distinction of green actinolite from colorless tremolite...*" (Leake et al. 1997). It appears that while the subdivisions were somewhat arbitrarily chosen to reflect changes in physical appearance, they are actually more meaningful. The selections of 10% ferro-actinolite for the division between tremolite and actinolite and 50% ferro-actinolite for the division between actinolite and ferro-actinolite were very appropriate because they mark distinct discontinuities in chemical and/or physical properties. We would further divide actinolite into two populations, with one population between 10 and 30% ferro-actinolite, and a second between 30 and 50% ferro-actinolite, for the same reasons.

Even given the comprehensive nature of these data, there are still critical deficiencies that limit the strength of our conclusions. First, there is a possibility for sampling bias based on the almost exclusive use of museum quality specimens. In particular, the presence of gaps or chemical discontinuities may be dependent on conditions of formation that are unique to museum quality specimens. We effectively increased our sample size by testing our major conclusions against the literature; however, the literature is likely to suffer from the same sampling bias. Second, the amount of F and Cl and the oxidation state of Fe in our samples are unknown. Third, we do not know the location and petrologic association of all the samples, and therefore could not assess their influence. These are clearly areas for future study, and we would certainly make any of our samples available for future investigations.

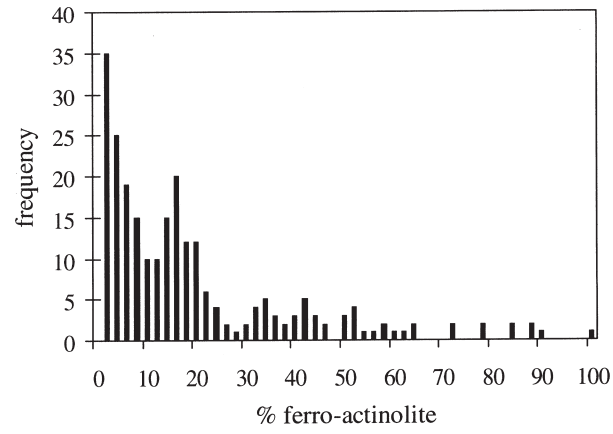

FIGURE 13. Frequency of samples in the actinolite series based on data from this work (103) samples, and from the literature (137 samples) and a bin size of 2% ferro-actinolite.

ACKNOWLEDGMENTS

For donating samples we thank the Smithsonian Institution (Museum of Natural History), Harvard Mineral Museum, the U.S. Bureau of Mines, Virginia Polytechnic Institute and State University, J.M.G. Davis, Bevan French, Jeff Furman, Dan Linder, G. B. Morey, Eric Steel, C.S. Thompson, Mark Watson, and Jim Webber. We thank Howard Evans for his help with the interpretation of X-ray diffraction data of ferro-actinolites. We greatly appreciate the help provided by Joe Conny in the use of principal component analysis and other methods of statistical analysis. Special thanks to Shirley Turner and E-an Zen for their careful reviews of the early stages of the manuscript, and to Bernard Evans and David Jenkins for their insightful reviews. Many thanks to John Armstrong for his general advice on electron microprobe analysis, and for his kind words and encouragement.

REFERENCES CITED

Bloss, F.D. (1981) The spindle stage: principles and practice, 340 p. Cambridge University Press, Cambridge, U.K.

Colville, P.A., Ernst, W.G., and Gilbert, M.C. (1966) Relationships between cell parameters and chemical compositions of monoclinic amphiboles. American Mineralogist, 51, 1727–1754.

Dana, E.S. (1932) A textbook of mineralogy, 4th Ed. revised by W.E. Ford, 574 p. Wiley, Inc, New York.

Deer, W. A., Howie, R.A., and Zussman, J. (1997) Rock-forming minerals, volume B, Double chain silicates, 2nd Ed., 764 p. The Geological Society, London.

Dorling, M. and Zussman, J. (1987) Characteristics of asbestiform and non-asbestiform calcic amphiboles. Lithos, 20, 469–489.

Ernst, W.G. (1966) Synthesis and stability relations of ferrotremolite. American Journal of Science, 264, 37–65.

———(1968) Amphiboles. Crystal chemistry, phase relations and occurrence, 125 p. Springer-Verlag, New York.

Evans, B.W. and Medenbach, O. (1997) The optical properties of cummingtonite and their dependence on Fe-Mg order-disorder. European Journal of Mineralogy, 9, 993–1003.

Evans, B.W. and Yang, H. (1998) Fe-Mg order-disorder in tremolite-actinolite-ferro-actinolite at ambient and high temperature. American Mineralogist, 83, 458–475.

Fiori, C.E. and Swyt, C. (1994) Desktop Spectrum Analyzer (DTSA). U.S. patent number 5,299,138, March 29.

Graham, C.M., Maresch, W.V., Welch, M.D., and Pawley, A.R. (1989) Experimental studies on amphiboles: a review with thermodynamic perspectives. European Journal of Mineralogy, 1, 535–555.

Hawthorne, F.C. (1981) Crystal chemistry of the amphiboles. In Mineralogical Society of America Reviews in Mineralogy, 9A, 1–102.

———(1995) Entropy-driven disorder in end-member amphiboles. The Canadian Mineralogist, 33, 1189–1204.

Hawthorne, F.C., Della Ventura, G., Robert, J., Welch, M.D., Raudsepp, M., and Jenkins, D.M. (1997) A Rietveld and infrared study of synthetic amphiboles along the potassium-richterite-tremolite join. American Mineralogist, 82, 708–716.

Heinrich, E.W. (1965) Microscopic identification of minerals, 414 p. McGraw-Hill Book Company, New York.

Jenkins, D.M. (1987) Synthesis and characterization of tremolite in the system H_2O-CaO-MgO-SiO_2. American Mineralogist, 72, 707–715.

Jenkins, D.M., Sherriff, B.L., Cramer, J., and Xu, Z. (1997) Al, Si, and Mg occupancies in tetrahedrally and octahedrally coordinated sites in synthetic aluminous tremolite. American Mineralogist, 82, 280–290.

Leake, B.E. (1968) A catalog of analyzed calciferous and subcalciferous amphiboles together with their nomenclature and associated minerals. Geological Society of America Special Paper 98.

——— (Ed.) (1978) Nomenclature of amphiboles. American Mineralogist, 63, 1023–1052.

Leake, B.E., Woolley, A.R., Arps, C.E.S., Birch, W.D., Gilbert, M.C., Grice, J.D., Hawthorne, F.C., Kato, A., Kisch, H.J., Krivovichev, V.G., et al. (1997) Nomenclature of amphiboles: Report of the subcommittee on amphiboles of the International Mineralogical Association, Commission on new minerals and mineral names. American Mineralogist, 82, 1019–1037.

Léger, A. and Ferry, J.M. (1991) Highly aluminous hornblende from low-pressure metacarbonates and a preliminary thermodynamic model for the Al content of calcic amphibole. American Mineralogist, 76, 1002–1017.

Marinenko, R.B. (1982) Preparation and characterization of K–411 and K–412 mineral glasses for microanalysis: SRM 470. NBS special publication 260–74, U.S. Department of Commerce, National Institute of Standards and Technology, Gaithersburg, MD 20899.

Materials Data, Inc. (1995) Jade for Windows: XRD pattern-processing for the PC. 1224 Concannon Blvd., Livermore, CA 94550.

Mitchell, J.T., Bloss, F.D., and Gibbs, G.V. (1971) Examination of the actinolite structure and four other *C*2/*m* amphiboles in terms of double bonding. Zeitschrift für Kristallographie, 133, 273–300.

National Institute of Standards and Technology (NIST) (1991) Certificate of analysis for standard reference material 1866a: Common commercial asbestos, Gaithersburg, MD, U.S.A.

Nesse, W. D. (1991) Introduction to optical mineralogy, 335 p. Oxford University Press, New York.

Papike, J.J., Ross, M., and Clark, J.R. (1969) Crystal-chemical characterization of clinoamphiboles based on five new structure refinements. Mineralogical Society of America Special Paper 2, 117–136.

Pawley, A.R., Graham, C.M., and Navrotsky, A. (1993) Tremolite-richterite amphiboles: Synthesis, compositional and structural characterization, and thermochemistry. American Mineralogist, 78, 23–35.

Philips Electronic Instruments Company (1991a) APPLEMAN least-squares cell parameters refinement program. 12 Michigan Dr., Natick, MA 01760.

———(1991b) POWDER: A program to calculate integrated X-ray diffraction intensities for polycrystalline materials from atomic structure information.12 Michigan Dr., Natick, MA 01760.

Phillips, W.R. and Griffen, D.T. (1981) Optical mineralogy: The nonopaque minerals, 677 p. W.H. Freeman and Company, San Francisco.

Saxena, S.K. and Ekström, T.K. (1970) Statistical chemistry of calcic amphiboles, Contributions to Mineralogy and Petrology, 26, 276–284.

Smelik, E.A., Jenkins, D.M., and Navrotsky, A. (1994) A calorimetric study of synthetic amphiboles along the tremolite-tschermakite join and the heats of formation of magnesiohornblende and tschermakite. American Mineralogist, 79, 1110–1122.

Robinson, P., Spear, F.S., Schumacher, J.C., Laird, J., Klein, C., Evans, B.W., Doolan, B.L. (1982) Phase relations of metamorphic amphiboles: Natural occurrence and theory. In Mineralogical Society of America Reviews in Mineralogy, 9B, 1–211.

U.S. EPA (1987) Asbestos-containing materials in schools: Final rule and notice. 40 CFR (Code of Federal Regulations) Part 763, Appendix A to Subpart F—Interim method of the determination of asbestos in bulk insulation samples. U.S. Government Printing Office.

Verkouteren, J.R., Steel, E.B., Windsor, E.S., and Phelps, J.M. (1992) Accuracy of the double variation technique of refractive index measurement. Journal of Research of the National Institute of Standards and Technology, 97, 693–705.

Yang, H. and Evans, B.W. (1996) X-ray structure refinements of tremolite at 140 and 295 K: Crystal chemistry and petrologic implications. American Mineralogist, 81, 1117–1125.

Winchell, A.N. (1945) Variations in composition and properties of the calciferous amphiboles. American Mineralogist, 28, 27–50.

Winchell, H. (1963) Clinoamphiboles regression studies, I. Regressions of optical properties and density on composition. Mineralogical Society of America Special Paper 1, 267–277.

Wylie, A.G. (1979) Optical properties of the fibrous amphiboles. Annals of the New York Academy of Science, 330, 600–605.

MANUSCRIPT RECEIVED FEBRUARY 26, 1999
MANUSCRIPT ACCEPTED APRIL 17, 2000
PAPER HANDLED BY ROBERTA OBERTI